

Electrochemical Polymerization of 1,4-Di(aryl)cyclopentadienes

By

Michael E. Vega

A dissertation submitted to the

Graduate School-Newark

Rutgers, The State University of New Jersey

In partial fulfillment of the requirements

For the degree of

Master of Chemistry

Graduate Program

Written under the direction of

Dr. Agostino Pietrangelo

And approved by

Newark, New Jersey

May, 2015

©2015

Michael E. Vega

ALL RIGHTS RESERVED

ABSTRACT OF THE DISSERTATION

Electrochemical Polymerization of 1,4-Di(aryl)cyclopentadienes

Dissertation Director:

Dr. Agostino Pietrangelo

A comparative study of the electrochemical polymerization of 1,4-di(aryl)-5,5-dimethylcyclopentadienes (XC5X) as a function of aryl group identity (X = thienyl, Th; furyl, Fur; and *N*-methylpyrrolyl; Pyr groups) is presented. The solubility of charged species generated at the surface of the working electrode during polymerization impedes efficient polymer growth and deposition with only ThC5Th and FurC5Fur monomers affording suitable films for analysis. Poly(ThC5Th) and poly(FurC5Fur) films possess a UV/vis absorption maxima λ_{max} of 500 nm and 400 nm, respectively, that when oxidized are bleached and give rise to low energy charge-carrier absorption features that are consistent with those observed in poly(terthiophene) and poly(terfuran), respectively. Addition of the anodically activated cross-linking agent 1,3,5-tris(2-aryl)benzenes (3XB) to a solution with XC5X greatly improved the formation of films. Spectroelectrochemical analyses reveal that copolymer films possess higher energy absorption signatures in both the neutral and oxidized state when compared to their corresponding homopolymer, a property attributed to the use of the meta-substituted arrangement of 3XB that is expected to reduce conjugation across the polymer backbone. A compositional variation study was performed comparing the ThC5Th:3ThB system to that of its aromatic congener terthiophene (Th₃), Th₃:3ThB. Based on the ThC5Th-containing systems, the optical

signatures of a film can be tailored towards poly(ThC5Th) by reducing the feed ratio of 3ThB in the comonomer solution. This indicates that film deposition can be improved by adding an additive without compromising the properties observed in the homopolymer.

Acknowledgement

Dr. Agostino Pietrangelo, thank you for allowing me to join your research group and to expand my knowledge of polymers as well as various chemical reactions and characterization. I never thought that I would be doing electrochemistry or spectroelectrochemistry. I had never heard of spectroelectrochemistry before and now I know a great deal about it. Under your guidance, we managed to get great results that told a nice story at the end of all this.

I'd like to thank all the members of the Pietrangelo group including Lei Chen, Rajani Bhat, Heta Patel, Xiao-li Sun, Curtis Casseus, Sufian Mahmoud, and Baris Yilmaz for answering my questions, helping me when I needed it and finding ways to pass the time in the lab. I'd especially like to thank Lei Chen for training me in the reactions that I needed and being there whenever I had a question. Without your help Lei, I wouldn't be where I am today.

Amir Khoshi: I appreciate all your help with AFM and SEM and teaching me how to use the instruments. Thanks for sitting with me in that hot AFM room all those afternoons so I could get my 3 data points for all 8 of my films.

Alex, James and Nick: I've had a blast every time I go into NYC to see you guys and appreciate that your couches are always available for me to crash on. I appreciate you guys asking about my research and waiting until I finished my first sentence before you told me you have no idea what I'm talking about.

Last but certainly not least, I'd like to thank my parents for all their support throughout graduate school and my life. You have enabled me to experience a lot of great things in my life and have pushed me to succeed.

List of Figures

Figure 1-1: Band gap	2
Figure 1-2: Aromatic to quinoid form using poly(thiophene)	2
Figure 1-3: Common π -conjugated polymers	3
Scheme 1-1: Mechanism of the electrochemical polymerization of poly(thiophene)	3
Figure 1-4: Ring opening of poly(furan)	5
Figure 1-5: Examples of 1,3,5-tris(aryl)benzenes	5
Figure 1-6: Fused Aromatic Ring Examples	6
Figure 1-7: Linear Olefinic Moiety Examples	7
Figure 1-8: Methano[10]annulene	8
Scheme 1-2: XC5X Synthesis	10
Scheme 1-3: Poly(fluorene-alt-cyclopentadiene) synthesis	11
Figure 1-9: Molecular wires bearing cyclopentadiene, thiophene & furan	12
Scheme 1-4: Electron oxidation of 1,4-bis-(2-thienyl)-1,3-cyclopentadiene	13
Scheme 1-5: Representation of electrochemical polymerization of XC5X & comonomer solution of XC5X:3XB	14
Figure 2-1: CV of XC5X & 10 scan polymerization of XC5X	15
Figure 2-2: CV of poly(XC5X) mono-free & spectroelectrochemistry	17
Figure 2-3: UV/vis of ThC5Th (drop-casted) & poly(ThC5Th)	18
Figure 2-4: UV/vis of FurC5Fur (drop-casted) & poly(FurC5Fur)	18
Figure 2-5: CV of 60:40 XC5X:3XB & 10 scan polymerization	21
Figure 2-6: CV of 60:40 poly(XC5X:3XB) mono-free & spectroelectrochemistry	23

Figure 2-7: UV/vis of ThC5Th, 3ThB (drop-casted) & poly(ThC5Th:3ThB)	24
Figure 2-8: UV/vis of PyrC5Pyr, 3PyrB & poly(PyrC5Pyr:3PyrB)	25
Figure 2-9: UV/vis of FurC5Fur, 3FurB & poly(FurC5Fur:3FurB)	26
Figure 2-10: 10 scan polymerization of ThC5Th (60:40, 75:25 & 90:10)	28
Figure 2-11: CV of poly(ThC5Th:3ThB) in monomer-free solution at 60:40, 75:25 & 90:10	29
Figure 2-12: UV/vis of poly(ThC5Th:3ThB) at 60:40, 75:25 & 90:10	30
Figure 2-13: Spectroelectrochemistry of poly(ThC5Th:3ThB) at 75:25 & 90:10	31
Figure 2-14: 10 scan polymerization of poly(Th ₃ :3ThB) at 60:40, 75:25 & 90:10	32
Figure 2-15: UV/vis of poly(Th ₃ :3ThB) at 60:40, 75:25 & 90:10	33
Figure 2-16: CV of poly(Th ₃ :3ThB) & spectroelectrochemistry at 60:40, 75:25 & 90:10	34
Figure 2-17: Pictures of the oxidized and reduced 60:40 films	35
Figure 2-18: SEM images of 60:40 poly(XC5X:3XB)	36
Figure A-1: CV of 3ThB	42
Figure A-2: CV of 3PyrB	42
Figure A-3: CV of 3FurB	43
Figure A-4: 10 scan polymerization of 3ThB	43
Figure A-5: 10 scan polymerization of 3PyrB	44
Figure A-6: 10 scan polymerization of 3FurB	44

List of Tables

Table 1-1: XC5X Data	11
Table A-1: Copolymer & monomer E_{on} and $E_{\text{p,a}}$ values	45

List of Abbreviations

HOMO: Highest Occupied Molecular Orbital

LUMO: Lowest Unoccupied Molecular Orbital

SCE: Saturated Calomel Electrode

EDOT: 3,4-ethylenedioxythiophene

DFT: Density Functional Theory

NICS: Nuclear-Independent Chemical Shift

NMR: Nuclear Magnetic Resonance

B3YLP: Method in DFT calculations

6-31G(d,p): basis set

6-311G(d,p): basis set

XC5X: generic formula with X= Th, thiophene, Fur, furan, or Pyr, *N*-methylpyrrole

UV/vis: Ultraviolet-visible

3XB: 1,3,5-tris(aryl)benzene with X= Th, thiophene, Fur, furan, or Pyr, *N*-methylpyrrole

CV: Cyclic Voltammogram

DCM: Dichloromethane

ITO: Indium tin oxide

TBAPF₆: Tetrabutylammonium Hexafluorophosphate

E_{on} : onset potential

$E_{\text{p,a}}$: anodic peak current

Pt: platinum

SEM: scanning electron microscope

Th₃: terthiophene

Table of Contents

Abstract	ii
Acknowledgment	iv
List of Figures	vi
List of Tables	viii
List of Abbreviations	ix
Chapter 1.0: Introduction	1
Chapter 1.1: π -conjugated polymers	1
Chapter 1.2: Strategies for Adding Polyene Character	6
Chapter 1.3: Cyclopentadiene	8
Chapter 1.4: Goals	14
Chapter 2.0: Results and Discussion	15
Chapter 2.1: Electrochemical Polymerization of XC5X	15
Chapter 2.2: Spectroelectrochemistry of poly(XC5X)	19
Chapter 2.3: Electrochemical Polymerization of XC5X:3XB	20
Chapter 2.4: Spectroelectrochemistry of poly(XC5X:3XB)	27
Chapter 2.5: Compositional Variation of Copolymers	28
Chapter 2.6: Polymer Films and Morphology	35
Chapter 2.7: Conclusions	37
Chapter 2.8: Experimental Section	39
Chapter 2.8.1: Materials and Equipment	39
Chapter 2.8.2: Electrochemistry	40
Chapter 2.8.3: Spectroelectrochemistry	40
Chapter 2.8.4: Synthesis of 1,3,5-tris(2'-N-methylpyrrolyl)benzene (3PyrB)	40
Appendix	42
Chapter 2.9: References	46
Chapter 3: Curriculum vitae	49

Chapter 1: INTRODUCTION

1.1: π -Conjugated Polymers

π -Conjugated organic polymers possess (opto)electronic properties that are attractive for a variety of device applications that include organic field-effect transistors,¹ light-emitting diodes,² electrochromic displays,³ sensors,⁴ photovoltaics,⁵ and thermoelectric generators.⁶ The discovery of conductive poly(acetylene) by Shirakawa, Heeger and MacDiarmid⁷ led to an interest in studying conductive polymers and their work was recognized with the Nobel Prize in Chemistry in 2000.⁸ When oxidized by a halogen such as chlorine, bromine or iodine, poly(acetylene) (Polymer **1** in Figure 1-3) goes from an insulating polymer to a conductive polymer possessing a conductivity of *ca.* 10^5 Sm^{-1} which approaches that of metals such as copper *ca.* 10^8 Sm^{-1} .⁹ In addition to its high conductivity, poly(acetylene) has a relatively small band gap ($E_g = 1.5 \text{ eV}$). The band gap refers to the difference in energy between the highest-occupied-molecular-orbital (HOMO) and the lowest-unoccupied-molecular-orbital (LUMO). As shown in Figure 1-1, the band gap decreases as more ethylenes are added to the chain. This is a result of the energy difference between consecutive π and π^* levels becoming smaller and smaller as the chain length increases until the π and π^* levels form a valence and conduction band, respectively. This makes conjugated polymers such as poly(acetylene) possess small band gap energy, making it easier to excite an electron from the HOMO to the LUMO in order to generate charge-carriers; this is important for (opto)electronic device performance.

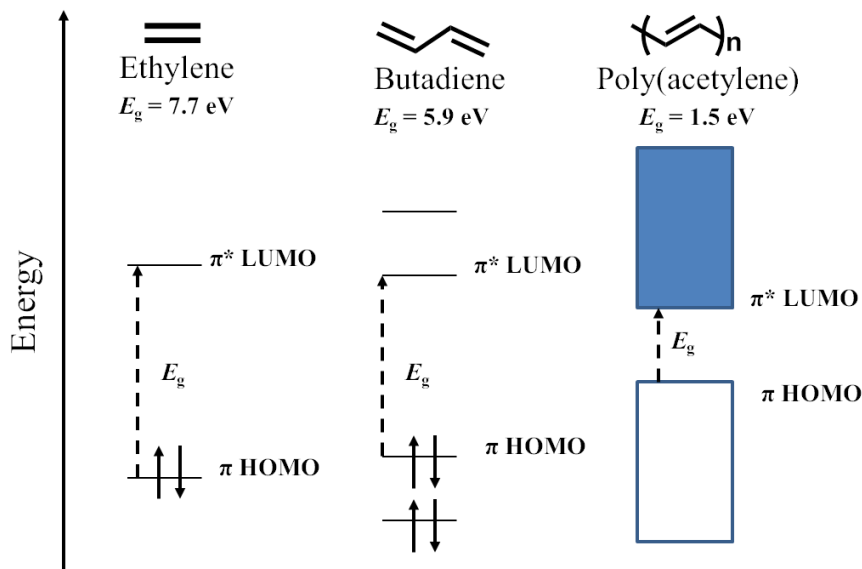


Figure 1-1: Diagram illustrating the band gap energy of ethylene, butadiene¹⁰ and poly(acetylene).

Unfortunately, poly(acetylene) is not very processable due to its insolubility. As an alternative, π -conjugated polymers being comprised of aromatic units¹¹ have been studied due to their environmental stability, processability, and chemical tunability. Key to the performance of these materials is their ability to undergo a distortion from the aromatic to quinoid structure (Figure 1-2) in order to stabilize charge-carriers generated under operationally-relevant scenarios.¹²

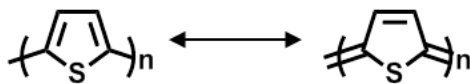


Figure 1-2: Formation of quinoid using poly(thiophene) 3.

Recently, computational studies have shown that increasing the aromaticity of the polymer backbone does not ensure a smaller band gap.¹³ This has led to great interest in introducing the polyene-character exhibited in poly(acetylene) to aromatic systems (*i.e.* poly(phenylene vinylene), Fig. 1-3; 2) as a means to destabilize their ground state

towards quinoid formation while enhancing the effective conjugation across the (macro)molecular backbone.¹⁴

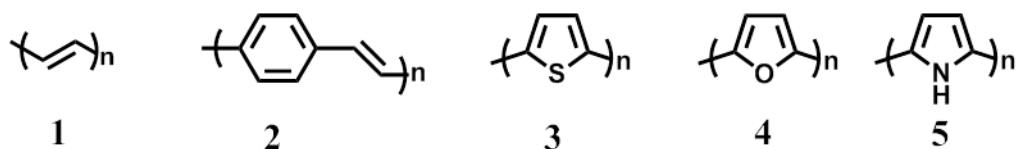
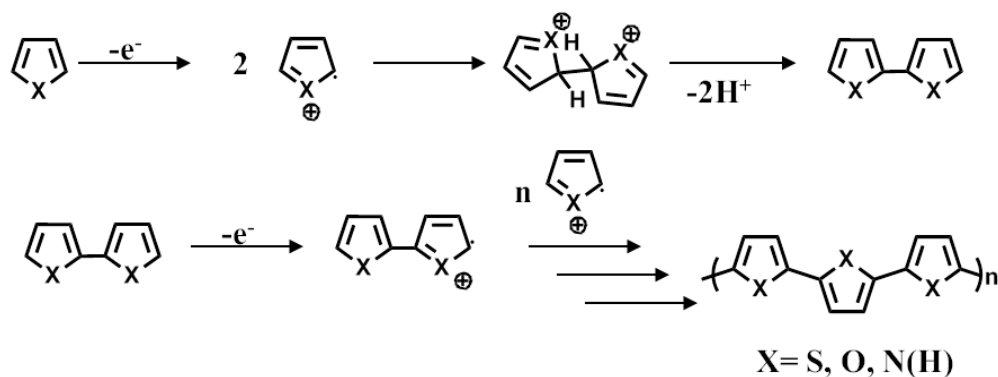


Figure 1-3: Examples of common π -conjugated polymers: poly(acetylene) **1**, poly(phenylene vinylene) **2**, poly(thiophene) **3**, poly(furan) **4**, and poly(pyrrole) **5**.

There has been an extensive body of work dedicated to the study of electrochemically-generated poly(thiophene)s¹⁵ (Fig. 1-3, **3**), poly(furan)s¹⁶ (Fig. 1-3, **4**), and poly(pyrrole)s (Fig. 1-3; **5**).¹⁷ In order for heterocyclic-containing polymers such as poly(thiophene) to have long effective conjugation length, a regular 2,5'-linked linear structure is needed.¹⁸ This can be done by electrochemical polymerization of the monomers shown in Scheme 1-1. The loss of an electron leads to the formation of a radical cation on the monomer. These cations combine to form a cationic dimer which loses two protons to form the neutral dimer. The dimer then loses an electron to form a cationic dimer which combines with a cationic monomer to form a trimer. This process repeats itself and results in a heterocyclic-containing polymer.



Scheme 1-1: Mechanism of the electrochemical polymerization of heterocyclic containing π -conjugated polymers.

To prevent overoxidation during film formation, poly(thiophene) has also been prepared from oligothiophenes such as bithiophene and terthiophene¹⁹ in order to lower the oxidation potentials required for polymerization. Through conventional chemical methods, alkyl substituents can be added to the β -position of the thiophene ring which can significantly increase the conjugation and conductivity compared to unsubstituted poly(thiophene).^{20,21} Alkyl groups are expected to decrease the oxidation potential of the polymer while increasing the crystallinity of the film for more densely packed polymers and the solubility for easier processability.²²

Poly(furan) has a band gap of 2.35 eV, which is higher than poly(thiophene) (2.0 eV) but lower than poly(pyrrole) (3.2 eV).²² Poly(furan) was made by electrochemical polymerization of furan; however, a high potential (*ca.* 1.8 V vs. SCE) was required and resulted in irreversible oxidation of the film.²³ In order to lower the oxidation potential, terfuran was selected as a monomer for electrochemical polymerization since terfuran has a lower oxidation potential than furan.²⁴ Glenis and coworkers, reported that the best poly(furan) films were made with the dopant anion, CF_3SO_3^- , which had the lowest anodic peak at 0.34 V (vs. SCE) suggesting that films made with this anion have the longest conjugation length and the least amount of ring opening. However, poly(furan) films made with the dopant anion PF_6^- or ClO_4^- had the shortest conjugation length and spectroscopic data suggest that a non-conjugated polymer was formed due to ring opening as shown in Figure 1-4.

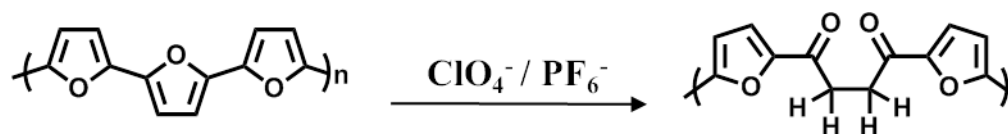


Figure 1-4: Potential pathway to ring opening by nucleophilic attack by the dopant and/or water on the positively charged α -carbon centers. Reproduced from Glenis, S.; Benz, M.; LeGoff, E.; Schindler, J. L.; Kannewurf, C. R.; Kanatzidis, M. G. *J. Am. Chem. Soc.* **1993**, *115*, 12519-12525.

Poly(pyrrole) was the first electrically conducting polymer film to be prepared by electrochemical polymerization.¹⁷ Poly(pyrrole) films are not very stable in air and begin to darken due to some oxidation after exposure to air. Derivatives of poly(pyrrole) became of interest in order to increase their stability in air. For example, adding substituents to the *N*-position make the polymers less sensitive to air; however, the conductivity of the film decreases drastically compared to poly(pyrrole) [poly(pyrrole): *ca.* 800 Sm^{-1} ; poly(*N*-methylpyrrole): *ca.* 0.1 Sm^{-1} .]

Electrochemistry has even been done for meta-substituted aromatic monomers such as 1,3,5-tris(aryl)benzenes.²⁵ Compounds containing thiophene, furan, and EDOT were synthesized via Stille cross-coupling reactions and the resulting 1,3,5-tris(aryl)benzenes are shown in Figure 1-5.

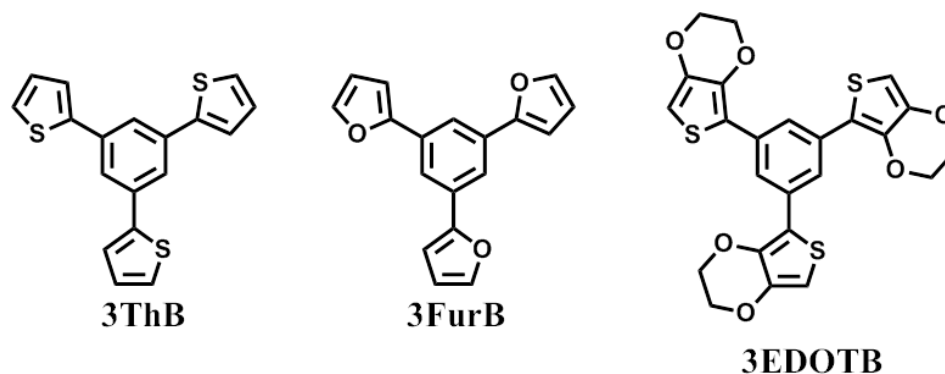


Figure 1-5: Examples of 1,3,5-tris(aryl)benzenes with the aryl groups being thiophene (Th), furan (Fur) and ethylenedioxythiophene (EDOT).

The resulting monomers were demonstrated to be electroactive and able to undergo electrochemical polymerization to form thin-films. The polymerization of 3FurB resulted in an oxidation peak that decreases after each subsequent scan. A reduction peak was not observed which indicates the formation of a poor conductive film on the surface of the electrode. 3ThB had a polymer peak that grows and shifts to a higher potential as the polymerization is taking place. The current stabilizes during the polymerization of 3ThB due to the poor conductivity of the film being formed and resulted in a black film deposited on the electrode.

1.2: Strategies for Adding Polyene Character

There are a few strategies that focus on adding polyene character to a π -conjugated system to promote quinoid formation. One such strategy uses fused aromatic rings with comparable resonance stabilization energies²⁶ where the aromatic character of one of the fused rings is used to reduce the aromaticity of the other ring. Examples of this strategy (Figure 1-6) being used are poly(benzo[c]-thiophene) **6**,^{26a} poly(2,3-dihexylthieno[3,4-b]pyrazine) **7**,^{26b} and poly(thieno[3,4-b]thiophene) **8**.^{26c} These types of π -conjugated polymers have been successful in reducing the band gap [*e.g.* poly(2,3-dihexylthieno[3,4-b]pyrazine) **7** $E_g = 0.95$ eV compared to poly(thiophene) $E_g = 2.0$ eV].^{26b}

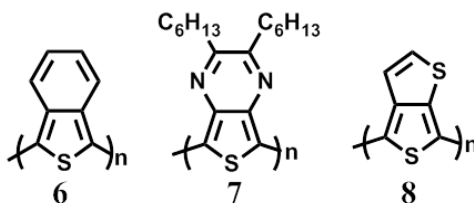


Figure 1-6: Examples of fused aromatic rings: poly(benzo[c]-thiophene) **6**, poly(2,3-dihexylthieno[3,4-b]-pyrazine) **7**, and poly(thieno[3,4-b]thiophene) **8**.

A second strategy employs the addition of linear olefinic moieties to aromatic species. Addition of ethylene linkages between thiophene rings leads to reduction in the rotational freedom between thiophene-thiophene bonds and a more planar geometry.²⁷ The ethylene linkage also decreases the overall aromaticity in the system as well as the band gap of poly(thiophene) **9** from 2.00 eV to 1.70 eV in poly(thiophene-vinylene) **10**.^{11a} However, addition of a butylene spacer between thiophene units, **11**, leads to a slight blue-shift *ca.* 3 nm when compared to poly(thiophene-vinylene). Therefore the addition of ethylene linkages can lower the overall aromaticity, however, the effectiveness of this strategy is limited due to an increase in the vibrational freedom in the system when multiple ethylene linkages are used.

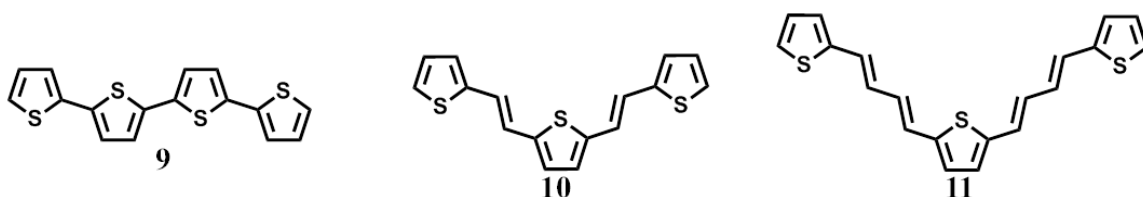


Figure 1-7: Examples of adding ethylene linkages.

Another strategy to reduce the aromaticity of π -conjugated polymers is to add more exotic species such as the aromatic methano[10]annulene subunit.^{14e,f, 28} The 10 π -electron methano[10]annulene subunit has enhanced intrapolymer delocalization compared to its congeners bearing a localized naphthalene unit. The authors attribute this phenomenon to the strong polyene character of the annulene. The UV/vis spectrum of the bithiophene-flanked annulene **12** (λ_{max} 420 nm) was shown to have a red-shifted λ_{max} compared to the bithiophene-flanked naphthalene unit **13** (λ_{max} 350 nm).

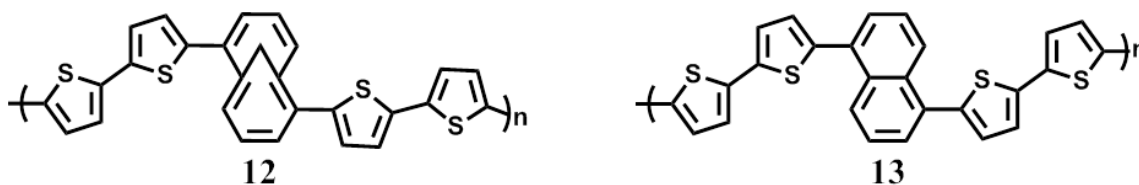


Figure 1-8: Bithiophene-flanked Methano[10]annulene **12** and bithiophene-flanked naphthalene **13**.

The peak anodic current ($E_{p,a}$) of the methano[10]annulene unit was lower than that of the naphthalene unit meaning that the HOMO level for annulene is higher and thus makes it easier to oxidize. The oxidation of the annulene unit appeared to be more electrochemically reversible than the naphthalene unit. The naphthalene-containing polymer possesses two strongly irreversible redox processes which suggest that the naphthalene unit has a more localized electronic structure. The spectroelectrochemical profiles of the annulene- and naphthalene-containing polymers were examined. The annulene polymer has a charge-carrier band centered at *ca.* 875 nm at moderate doping levels while the naphthalene-containing polymer had a narrower charge-carrier band blue-shifted by *ca.* 225 nm. This data suggests the theory that the annulene unit is more delocalized and has a longer effective conjugation length when compared to naphthalene.

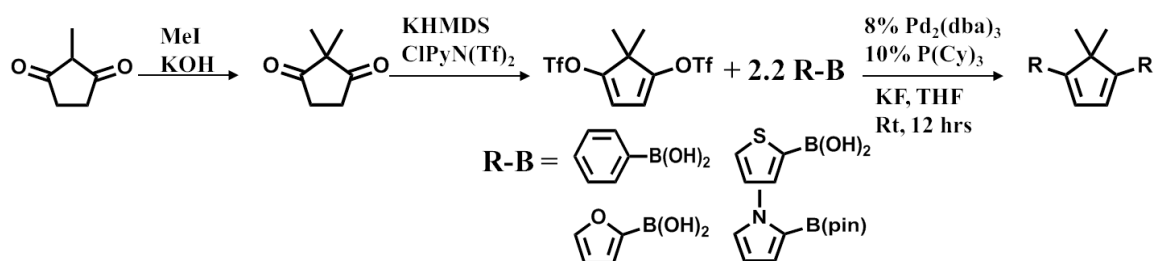
1.3: Cyclopentadiene

An attractive approach to adding polyene character into π -conjugated systems is through incorporating cyclopentadiene(s). The cyclopentadiene moiety shares a similar cyclic structure with common aromatics (*i.e.* thiophene, furan and *N*-methylpyrrole) present in π -conjugated polymers but does not possess resonance stabilization energy required to break aromaticity. In DFT studies by Cordaro and Wong,¹³ poly(cyclopentadiene-*alt*-vinylene) had its ground state calculated to be in the quinoidal

form which makes cyclopentadiene a candidate to decrease the aromaticity in π -conjugated polymers. Schleyer and coworkers utilized Nucleus-Independent Chemical Shift (NICS) to compute the diamagnetic and paramagnetic effect of ring currents and associate them with aromaticity or antiaromaticity (*i.e.* shielding and deshielding of nuclei) by assigning a NMR chemical shift.²⁹ NICS data are reported with the reverse signs in order to conform to the conventional NMR chemical shift where the negative values are for bonds more upfield and positive values are for bonds more downfield. Functional groups such as olefins and acetylenes as well as C-H and C-C single bonds influence their magnetic environments and thus affect the NMR.³⁰ The local effects of the sigma C-C and C-H influence the NICS(0) value of benzene but results in nonzero values for nonaromatic, saturated, and unsaturated hydrocarbon rings.³¹ These nonzero values using NICS(0) values led Schleyer and coworkers to suggest using a different method, namely, NICS(1). The measurements for NICS(1) values are taken 1 Å above the ring center in order to minimize the local effects of sigma C-C and C-H bonds compared to the ring current effects.³² They hope that this change in where the values are calculated at leads to more accurate numbers and better serves as an index for aromaticity. Corrado and Wong, used B3YLP/6-31G(d,p) to optimize the geometries of heterocyclic nonamers but then used the larger basis set 6-311G(d,p) to calculate NICS(1). To have NICS(1) values more representative of a polymer chain, the middle unit of the nonamer was used to calculate NICS(1) values. NICS(1) values provide a comparison of the aromaticity of the polymers studied with the more negative values denoting more aromatic species. For example, poly(pyrrole) has a very negative NICS(1) value (*ca.* -8.2 ppm) and therefore is aromatic. On the other hand, poly(cyclopentadiene) has a more positive NICS(1) value *ca.*

-3.0 ppm and is quinoidal. These calculations show that cyclopentadiene has the desired polyene character in its ground state.

Recently, the Pietrangelo group reported on a convenient route to a bifunctional (triflate and boronic ester) 5,5-dimethylcyclopenta-1,3-diene. 1,4-[bis(trifluoromethanesulfonyl)-oxy]-5,5-dimethylcyclopenta-1,3-diene undergoes a Suzuki-Miyaura cross-coupling reaction with aryl boronic acids (esters) under mild conditions to give a series of aryl/dienyl hybrids XC5X (X= Th, Fur, Pyr and Ph) in good-to-excellent yield. (Scheme 1-2).³³



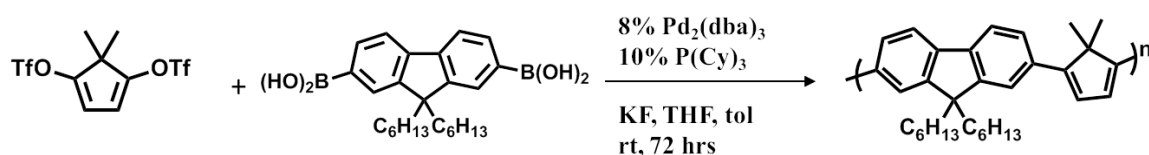
Scheme 1-2: Synthesis of XC5X monomers. Reproduced from Chen, L.; Mahmoud, S. M.; Yin, X.; Lalancette, R. A.; Pietrangelo, A. *Org. Lett.* **2013**, 15, 5970-5973.

When comparing XC5X with their aromatic congeners X₃, the cyclopentadiene moiety was found to reduce the HOMO-LUMO energy gap of the system while shifting the frontier orbital energies by an extent that is dependent on the aryl-group.

Entry	Aryl/dienyl hybrid	λ_{\max}^a	λ_{em}^b	E_{ox}^c	Yield	Entry	Aromatic congener	λ_{\max}^a	λ_{em}^b	E_{ox}^c
1	Ph-C5-Ph	340	420	1.12	85	5	Ph-Ph-Ph	279	342	1.84
2	Th-C5-Th	386	457	0.98	98	6	Th-Th-Th	355	429	1.29
3	Fur-C5-Fur	367 ^d	429 ^d	0.78 ^d	95	7	Fur-Fur-Fur	329 ^e	371 ^e	0.75 ^e
4	Pyr-C5-Pyr	355	447	0.50	81	8	Pyr-Pyr-Pyr	276 ^f	-	0.06 ^f

Table 1-1: ^aUV/vis absorption maximum, λ_{\max} (nm), in dichloromethane (CH_2Cl_2). ^bEmission maximum, λ_{em} in CH_2Cl_2 . ^cOxidation potential, E_{ox} (V vs. SCE), in CH_2Cl_2 containing 0.1M tetrabutylammonium hexafluorophosphate. ^dData acquired in acetonitrile (CH_3CN). ^eData obtained from ref 24 & 34. ^fData obtained from ref 35. Reproduced from Chen, L.; Mahmoud, S. M.; Yin, X.; Lalancette, R. A.; Pietrangelo, A. *Org. Lett.* **2013**, 15, 5970-5973.

This synthetic methodology was then extended to chemically prepare a poly(fluorene) derivative bearing alternating cyclopentadiene repeat units which was the first of its kind prepared in this manner.



Scheme 1-3: Synthesis of poly(fluorene-alt-cyclopentadiene). Reproduced from Chen, L.; Mahmoud, S. M.; Yin, X.; Lalancette, R. A.; Pietrangelo, A. *Org. Lett.* **2013**, 15, 5970-5973.

This polymer was found to have UV/vis absorption and emission maxima that are red-shifted when compared to a poly(fluorene-*alt*-thiophene) derivative of comparable molecular weight. This is consistent with what was observed for XC5X small molecules and confirms that substituting aromatic repeat units in polymers with cyclopentadiene can also shift the frontier orbital energy gap of polymers. In an independent study,³⁶ Breslow

and coworkers have shown that substituting aromatic units (*e.g.* furyl, and thienyl) with cyclopentadiene **14** (Figure 1-9) resulted in higher conductance in single-molecule junction for molecular wires compared to thiophene **15** and furan **16** containing wires. This work further supports the potential utility of incorporating cyclopentadienes into π -conjugated systems.

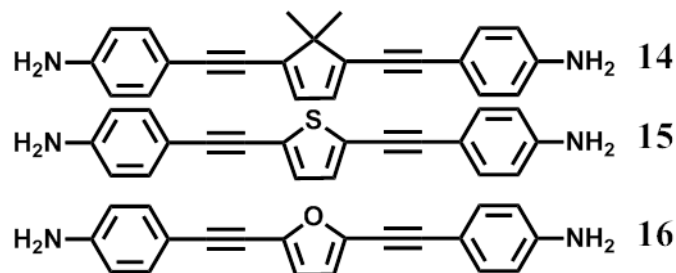
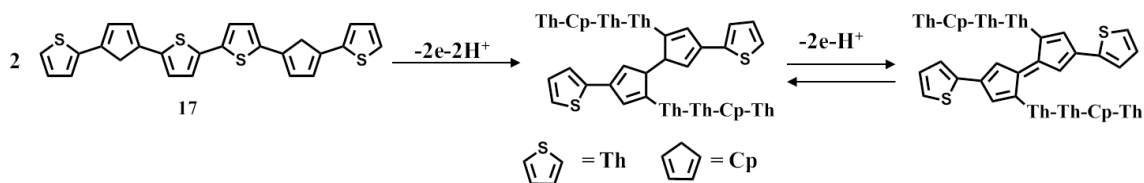


Figure 1-9: Molecular wires with cyclopentadiene **14**, thiophene **15**, and furan **16**.

Since the monomers of poly(thiophene), poly(furan) and poly(pyrrole) are structurally similar to XC5X prepared in our laboratory, there was interest in anodically polymerizing XC5X onto conductive substrates to examine how the aryl group influences the electrochemical, optical, spectroelectrochemical, and morphological properties of electrochemically-generated cyclopentadiene-containing polymers. Electrochemical polymerization is a useful method for the preparation of π -conjugated systems for structure/property correlation studies³⁷ and offers several advantages over the conventional chemical methods including: i) facile polymer purification due to the absence of transition metal catalysts and other additives that are required in typical chemical reactions, ii) the ability to directly grow a polymer film onto a conductive substrate for characterization, and iii) thin-film thickness and morphology control due to the selection of substrate, electrolyte, potential, and solvent.^{14,38}

To date, only ThC5Th has been anodically polymerized affording a partially soluble polymer film in a dark blue bulk solution due to the presence of soluble radical cationic oligomers formed at the working electrode.³⁹ Schiavon and co-workers investigated the polymerization of dithienylcyclopentadiene, Th-Cp-Th, by anodic coupling in acetonitrile. They found that with the unsubstituted dithienylcyclopentadiene dimer **17**, there was coupling at both the alpha-position of the thiophenes as well as at the 5-position of the cyclopentadiene which formed an insoluble polymer as shown in Scheme 1-4. The undesired coupling at the 5 position of the cyclopentadiene is due to the acidic hydrogens present at this position so protection of the 5 position with alkyl groups would prevent this coupling.

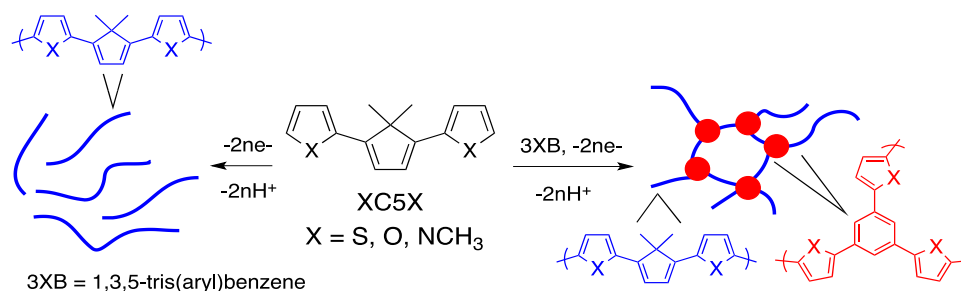


Scheme 1-4: Electron oxidation of 1,4-bis-(2-thienyl)-1,3-cyclopentadiene. Reproduced from Berlin, A.; Zotti, G.; Zecchin, S.; Schiavon, G. *Macromol. Chem. Phys.* **2002**, 203, 1228-1237.

When the cyclopentadiene was protected with alkyl groups at the 5-position, coupling only occurred at the alpha-positions of the thiophenes. Poly(5,5-dimethyl-1,4-bis(thien-2-yl)-1,3-cyclopentadiene) has an optical band gap of 2.3 eV and a conductance *in situ* value of 800 Sm⁻¹ which are close to those observed in poly(thiophene) (2.3 eV and 1000 Sm⁻¹).⁴⁰ The cyclopentadiene moiety was found to be similar to the thiophene ring and does not interfere with the electronic properties of the conjugated chain.

1.4: Goals

To the best of our knowledge, a thorough analysis of the properties of this exciting class of polymer and their comparison to common aromatic systems has yet to be explored. We set out to confirm the small molecule study of the XC5X species previously conducted by the Pietrangelo group³³ applies to their respective homopolymer, poly(XC5X) by using UV/vis spectroscopy and spectroelectrochemistry to determine their effective conjugation length and charge-carriers. Additionally, we set out to polymerize XC5X in the presence of an additive to promote polymer film formation by impeding the dissolution of oligomers into the bulk electrolyte solution seen by Schiavon and coworkers when electrochemically polymerizing ThC5Th.³⁹ We report on the synthesis and characterization of films prepared from the copolymerization of XC5X and 1,3,5-tris(2-aryl)benzenes, electroactive monomers²⁵ that are exploited as anodically activated cross-linking agents (Scheme 1-5). Structure/property correlations based on the identity of the aryl group and comonomer composition are also discussed.



Scheme 1-5: Left: Homopolymerization of XC5X monomers. Right: Copolymerization of XC5X and 3XB.

Chapter 2: RESULTS AND DISCUSSION

2.1: Electrochemical Polymerization of XC5X

In order to determine a potential window that enables electropolymerization, the electrochemistry of each monomer was investigated. The cyclic voltammograms of XC5X are shown in Figure 2-1a and exhibit features that are consistent with multistep redox processes occurring between *ca.* -1.0 and 1.5 V (*vs.* Fc/Fc⁺). When the potential window only encompassed the first redox wave of the monomer, there was no film growth observed during cycling. The characteristics indicative of electrochemical polymerization and thin-film formation⁴¹ (*i.e.* anodic peak increase in current and shift to higher potentials) were only observed when XC5X solutions had a potential window that was swept between *ca.* -0.5 and 1.5 V (scan rate, 100 mV/s, 10 cycles, Figures 2-1b-d).

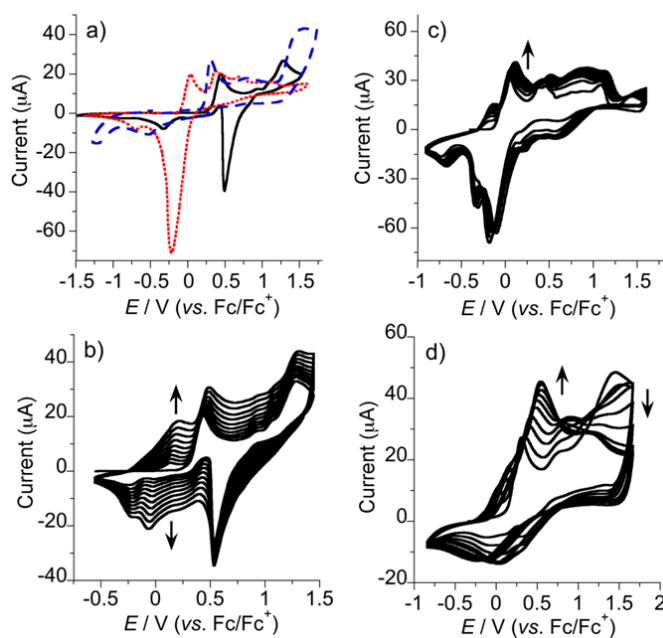


Figure 2-1: a) First CV scans of XC5X solutions: ThC5Th, black line; PyrC5Pyr, red dotted line; FurC5Fur, blue dashed line. CV scans (10 cycles) of b) ThC5Th, c) PyrC5Pyr, and d) FurC5Fur solutions. Conditions: Monomer concentration, 4.2 mM in 0.1 M [n-Bu₄N]PF₆ in DCM; scan rate, 100 mV/s, Pt disc working electrode, *E* *vs.* Fc/Fc⁺.

A comparative analysis between the CVs clearly shows that the ThC5Th monomer (Figure 2-1b) electrochemically polymerizes more effectively than its *N*-methylpyrrolyl (Figure 2-1c) and furyl (Figure 2-1d) congeners as made apparent by the consistent and gradual growth of the poly(ThC5Th) redox wave at 0.22 V. The PyrC5Pyr monomer exhibits little growth of a poly(PyrC5Pyr) redox wave at -0.2 V but this does not result in a film being deposited onto the surface of the electrode. FurC5Fur exhibits better polymerization than PyrC5Pyr as made evident by the growth of the poly(FurC5Fur) redox wave at *ca.* 0.07 V with film being deposited onto the surface of the working electrode. The dark bulk solutions of the PyrC5Pyr and FurC5Fur systems (and to a lesser extent ThC5Th) during polymerization are consistent with observations reported by Berlin and coworkers,³⁹ which suggest that the anodically generated oligomers are too soluble for efficient electrochemical deposition. Therefore, only monomers ThC5Th and FurC5Fur afforded polymer films that were suitable for further investigation.

Poly(ThC5Th)- and poly(FurC5Fur)-modified Pt-disc electrodes were rinsed thoroughly with DCM and placed in monomer-free electrolyte solutions for additional CV studies (Figures 2-2a and 2-2b).

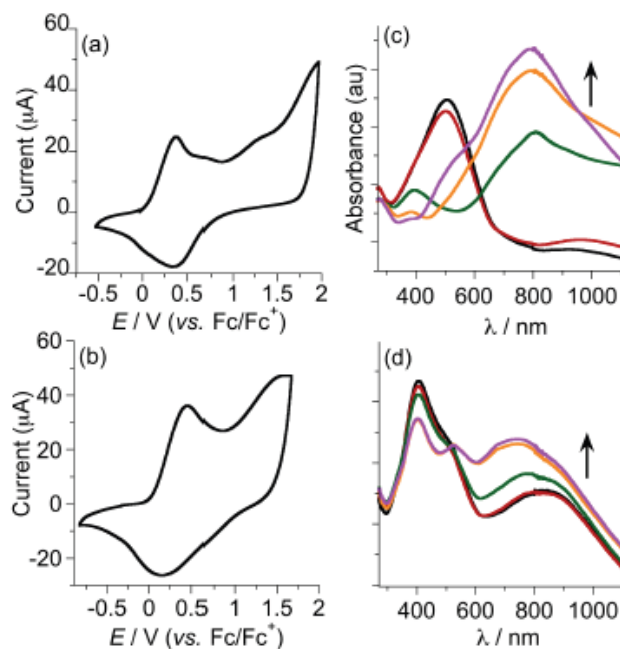


Figure 2-2: CV scans (in monomer-free electrolyte) of (a) poly(ThC5Th) and (b) poly(FurC5Fur) deposited onto a platinum disc electrode. Spectroelectrochemical profiles of (c) poly(ThC5Th) and (d) poly(FurC5Fur) held between *ca.* 0.0 V and 1.20 V and *ca.* 0.8 V and 1.4 V, respectively. All spectra were obtained from a film grown on an ITO-coated electrode. The black UV/Vis/NIR spectrum was taken from the film in their neutral state. All subsequent spectra (*i.e.* red, green, orange and violet) were taken at progressively higher potentials at 400 mV intervals for poly(ThC5Th) and 200 mV for poly(FurC5Fur) over the ranges indicated above.

The monomer, ThC5Th, possesses an onset of oxidation potential E_{on} (*ca.* 0.32 V vs. Fc/Fc⁺) that is *ca.* 320 mV higher than the E_{on} of the poly(ThC5Th), indicating that the polymer has a longer effective conjugation length than the monomer. This observation is supported by the UV/vis absorption spectrum of poly(ThC5Th) deposited on ITO (Figure 2-3). Poly(ThC5Th) has a λ_{max} at 500 nm that is bathochromically shifted by *ca.* 108 nm to that of a drop-casted film of ThC5Th. The broad π - π^* transition band observed is due to the intrinsic energetic disorder in the film from variations in conjugation length among the polymer segments.⁴²

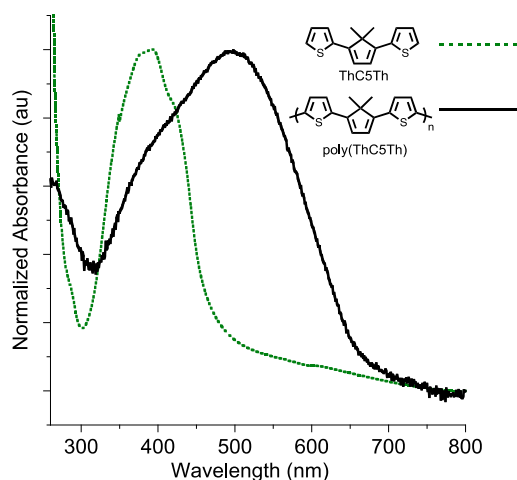


Figure 2-3: UV/vis absorbance spectra of ThC5Th (drop casted film on ITO) and poly(ThC5Th) (electrochemically generated film on ITO).

Neutral films of electrochemically-generated poly(terthiophene) and poly(thiophene) have a higher energy λ_{max} *ca.* 400 and 485 nm respectively,¹⁹ when compared to poly(ThC5Th). These observations are consistent with those from our previous report showing that cyclopentadiene moieties reduce the optical band of π -conjugated organic polymers when supplanting aromatic units in the (macro)molecular scaffold.³³

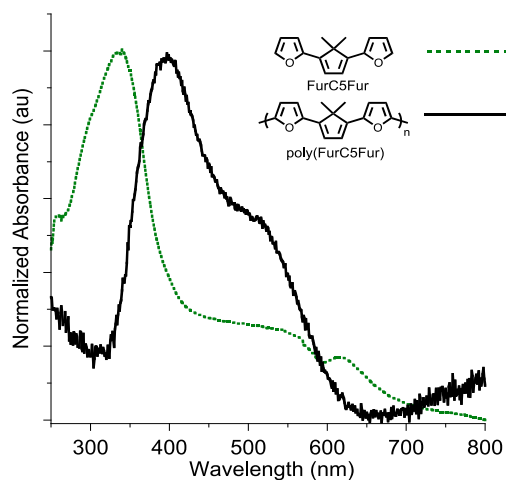


Figure 2-4: UV/vis absorbance spectra of FurC5Fur (drop casted film on ITO) and poly(FurC5Fur) (electrochemically generated film on ITO).

On the other hand, poly(FurC5Fur) films exhibit a λ_{max} (*ca.* 395 nm, Figure 2-4) that is hypsochromically shifted by *ca.* 73 nm with respect to electrochemically-generated poly(terfuran). This hypsochromic shift can be attributed to the use of the dopant ion PF_6^- during the polymerization of poly(FurC5Fur) which has been known to damage the conjugation structure and reduce the conjugation length in poly(furan)s²⁴ and/or by the large overpotentials necessary during electropolymerization that can break the conjugated backbone due to over-oxidation of the polymer film.⁴³ Poly(FurC5Fur) possesses a low energy band extending into the near-IR region indicating the incomplete reduction of the polymer film. This can be seen in the CV features shown in Figure 2-1d where the oxidation of FurC5Fur (at 0.3 V, cycle 1) progressively shifts to higher potentials after successive sweeps with little polymer growth (*ca.* 0.07 V) observed, a consequence that can be attributed to the greater overpotentials required to overcome the electrical resistance of the poly(FurC5Fur) film. Despite these results, it appears that longer conjugation lengths are present in the homopolymer since both the E_{on} (0.0 V) and λ_{max} values of poly(FurC5Fur) are lower than that of the monomer FurC5Fur (*ca.* 0.2 V and 335 nm respectively).

2.2: Spectroelectrochemistry of poly(XC5X)

Spectroelectrochemical analyses of poly(XC5X) films grown on ITO were performed to examine charge-carrier evolution during oxidation in 0.1 M TBAPF₆/DCM (Figure 2-2).⁴⁴ The neutral film of poly(ThC5Th) shows a π - π^* transition band λ_{max} at 500 nm. Stepwise oxidation of poly(ThC5Th) results in the bleaching of this π - π^* transition band and the generation of a broad low-energy polaronic charge-carrier band (λ_{max} = 800 nm) that increases in intensity at progressively higher potentials. These

optical signatures are in line with the spectroelectrochemistry of high quality electrochemically-generated poly(thiophene) films.⁴⁵ Poly(FurC5Fur) has a π - π^* transition band λ_{max} of 406 nm for the neutral film. Only a modest reduction in the poly(FurC5Fur) π - π^* transition band is observed over a comparable potential range, and growth of a charge-carrier band that shifts slightly to higher energies (*ca.* 740 nm) upon application of greater positive potentials is observed. Poly(terfuran) films characterized in the same electrolyte solution have also observed this phenomenon.⁴⁶ These results for poly(ThC5Th) and poly(FurC5Fur) suggest that the cyclopentadiene moiety influences the energy of the optical transitions of poly(XC5X) films in the neutral and doped states while charge-carrier evolution is similar to their aromatic congeners, poly(thiophene) and poly(terfuran), respectively.

2.3: Electrochemical Polymerization of XC5X:3XB

The electrochemistry of 1,3,5-tris(2-aryl)benzenes (Figures A-1- A-3) was reexamined²⁵ to determine whether CV would be an effective means to prepare random copolymers from XC5X and 3XB. All of the cross-linking monomers exhibited limited polymer growth under our conditions (Figures A-4- A-6) with polymer film growth seen at the working electrode. The 3XB monomers had higher onset potentials E_{on} (Table A-1) than their respective XC5X systems which means XC5X is the monomer that is more easily oxidized in the comonomer solution. Moreover, E_{on} values of XC5X and 3XB differ by only *ca.* 0.1 - 0.5 V indicating that oxidative coupling between comonomer species is viable without excessive overpotentials that are known to promote mis-linkages that stray from the ideal 2,5' linkages *i.e.* 2,3 linkages and oxidative degradation.⁴⁷ Several molar ratios of XC5X:3XB were surveyed to see how feasible the use of 3XB

would be as a second monomer to enhance polymer film deposition. The molar ratio of 60:40 XC5X:3XB was selected for further study as this ratio lead to polymer film formation suitable for further analysis in all the systems. The first scan cyclic voltammograms of 60:40 comonomer XC5X:3XB solutions are illustrated in Figure 2-5a. The CVs possess features consistent with those observed for their individual monomer components, XC5X and 3XB, which indicates that E_{on} is a result of the oxidation of XC5X.

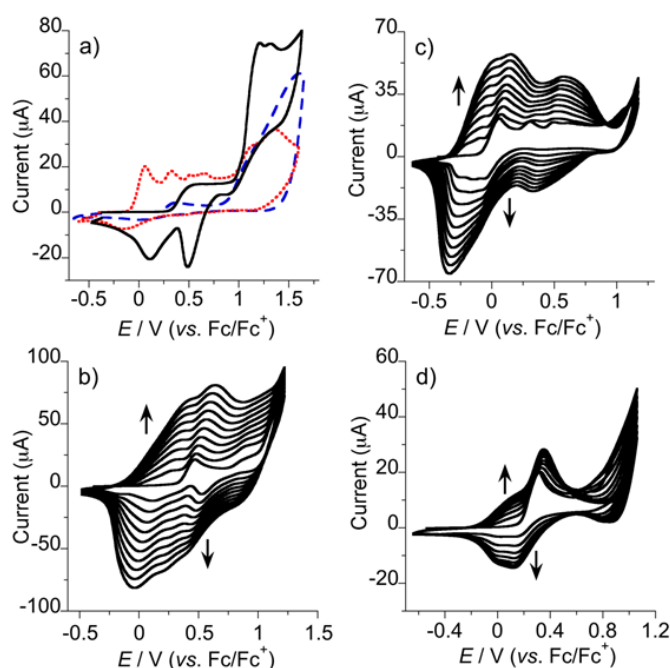


Figure 2-5: a) First CV scans of XC5X:3XB (60:40) comonomer solutions: ThC5Th:3ThB, black line; PyrC5Pyr:3PyrB, red dotted line; FurC5Fur:3FurB, blue dashed line. CV scans (10 cycles) of b) ThC5Th:3ThB, c) PyrC5Pyr:3PyrB, and d) FurC5Fur:3FurB (60:40) comonomer solutions. Conditions: concentration of electropolymerizable species, 4.2 mM in 0.1 M $[n-Bu_4N]PF_6$ in DCM; scan rate, 100 mV/s, Pt disc working electrode, E vs. Fc/Fc^+ .

A potential window for each set of comonomers was selected based on their E_{on} and peak anodic current potentials ($E_{p,a}$, Table A-1) to ensure that both monomers were

oxidized during electrochemical polymerization due to the features of the comonomer cyclic voltammograms being dependent upon the aryl-group (*i.e.*, X = S, O, or N(Me)) being used.

The cyclic voltammograms of ThC5Th:3ThB, PyrC5Pyr:3PyrB, and FurC5Fur:3FurB (60:40) solutions through 10 cycles are shown in Figures 2-5b-d. Both monomers are incorporated into the insoluble copolymer film since the cyclic voltammograms have little resemblance to those obtained from solutions of the individual monomer components (Figures 2-1b-d, and Appendix). All of the comonomer systems (particularly, the Pyr-containing derivative, Figure 2-5c) show enhanced increases in peak-current that shift to higher oxidation potentials when 3XB is present in solution. Notably, the Pyr-containing derivative (Figure 2-5c) exhibits enhanced electrochemical polymerization compared to the homopolymer where no film growth was observed confirming that the cross-linker, 3XB, facilitates polymer deposition. The FurC5Fur:3FurB system was scanned at the smallest potential window compared to the other systems due to over-oxidation of the film at higher potentials. The ThC5Th:3ThB and PyrC5Pyr:3PyrB systems had potential windows that went beyond the anodic peak current of their respective cross-linker. Moreover, the anodic peak currents of ThC5Th:3ThB and PyrC5Pyr:3PyrB increase more rapidly during copolymerization compared to the FurC5Fur:3FurB system implying that polymer growth is slower in the latter.⁴⁸ This slow polymer growth in the FurC5Fur:3FurB system would explain why poly(FurC5Fur:3FurB) films are the thinnest (27 ± 3 nm) of the poly(XC5X:3XB) films with poly(ThC5Th:3ThB) (75 ± 17 nm) and poly(PyrC5Pyr:3PyrB) (77 ± 6 nm) having thicker films grown under identical conditions. The thin film of poly(FurC5Fur:3FurB)

also explains why the electrolyte solution of FurC5Fur:3FurB turned purple after each CV experiment, which is due to soluble low-molecular weight products that diffuse away from the working electrode surface.

Poly(XC5X:3XB) films deposited on Pt-disc electrodes exhibit quasi-reversible anodic behavior (Figure 2-6a-d) in monomer-free electrolyte solutions with well-defined features that are unique to the identity of the aryl-group moieties.

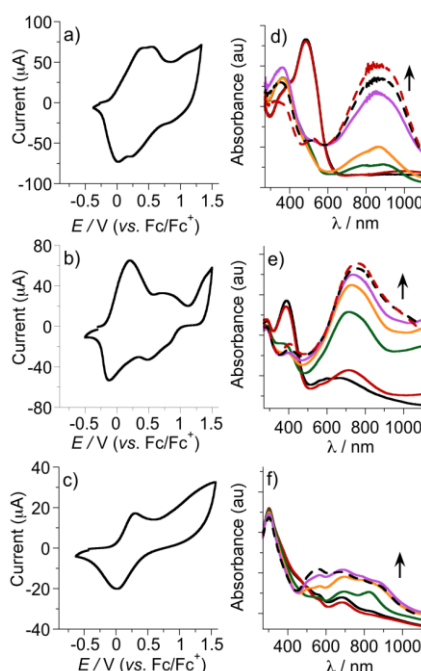


Figure 2-6: CV scans (in monomer-free electrolyte) of: a) ThC5Th:3ThB, b) PyrC5Pyr:3PyrB, c) FurC5Fur:3FurB, and d) Th₃:3ThB random copolymers deposited onto a platinum disc electrode. All copolymers were prepared from XC5X:3XB (60:40) comonomer solutions under conditions described in Figure 1. Spectroelectrochemical profiles of: e) ThC5Th:3ThB, f) PyrC5Pyr:3PyrB, and g) FurC5Fur:3FurB h) Th₃:3ThB random copolymers held between *ca.* -0.10 V and 0.90 V, *ca.* -0.30 V and 0.7 V, *ca.* -0.10 V and 0.70 V, *ca.* 0.3 V and 1.3 V, respectively. All spectra were obtained from films grown on ITO-coated electrodes. All black UV/Vis/NIR spectra were taken from films in their neutral state. All subsequent spectra (*i.e.* red, green, orange, violet, black dashed, and red dashed lines) were taken at progressively higher potentials at 200 mV intervals over the ranges indicated above.

The largest difference between comonomer and copolymer E_{on} values (Table A-1) was observed between ThC5Th:3ThB and poly(ThC5Th:3ThB). This suggests that the effective conjugation lengths of the thiophene-containing cross-linked copolymer networks are more extended than those observed in their *N*-methylpyrrolyl and furyl congeners. UV/vis absorption spectra of the copolymer films on ITO substrates were compared against drop-casted films of their individual monomer components (Figure 2-7- Figure 2-9) and homopolymer analogs where available to further investigate this observation.

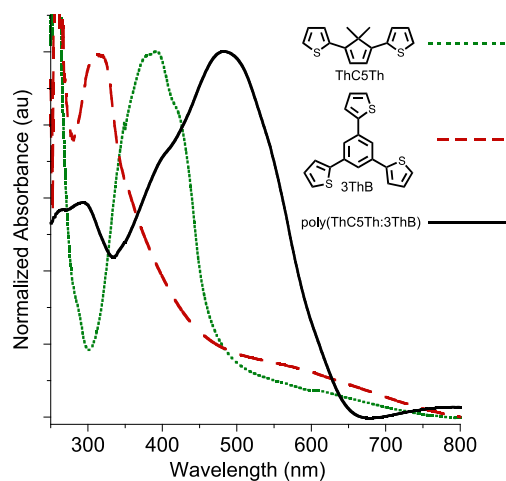


Figure 2-7: UV/vis absorbance spectra of ThC5Th (drop casted film on ITO), 3ThB (drop casted film on ITO), and poly(ThC5Th:3ThB, 60:40) (electrochemically generated film on ITO).

Poly(ThC5Th:3ThB) possesses a π - π^* transition band with a λ_{max} of 482 nm (Figure 2-7) that is *ca.* 90 and 169 nm red-shifted from the absorption maxima of ThC5Th and 3ThB, respectively. There is a high-energy shoulder centered at *ca.* 300 nm that is absent in the spectrum of poly(ThC5Th) but in line with λ_{max} of 3ThB (*ca.* 315 nm) suggesting that 3ThB is incorporated into the polymer. The π - π^* transition band of poly(ThC5Th:3ThB) is hypsochromically shifted compared to that of poly(ThC5Th),

which is attributed to the meta-substituted arrangement of the cross-linking 3ThB junction that is expected to reduce conjugation along the cross-linked macromolecular scaffold.

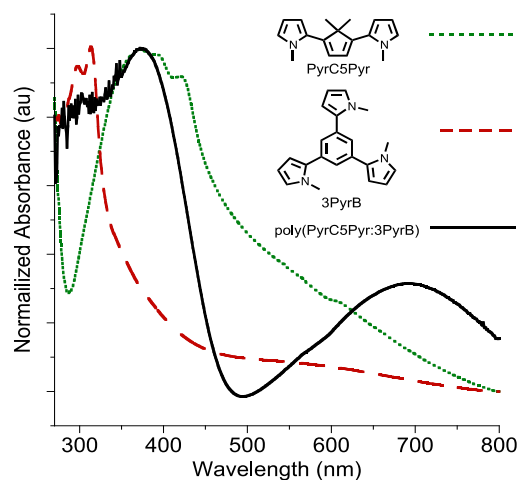


Figure 2-8: UV/vis absorbance spectra of PyrC5Pyr (drop casted film on ITO), 3PyrB (drop casted film on ITO), and poly(PyrC5Pyr:3PyrB) (electrochemically generated film on ITO).

Poly(PyrC5Pyr:3PyrB) has a π - π^* transition band with a λ_{max} of 376 nm (Figure 2-8) as well as a broad absorption band at *ca.* 694 nm which is indicative of incomplete reduction. The π - π^* band is red-shifted by *ca.* 19 nm and 71 nm from the λ_{max} of PyrC5Pyr and 3PyrB, respectively. Again, a high energy shoulder is seen at *ca.* 300 nm which is close to the λ_{max} of 3PyrB which would suggest that 3PyrB has been incorporated into the film.

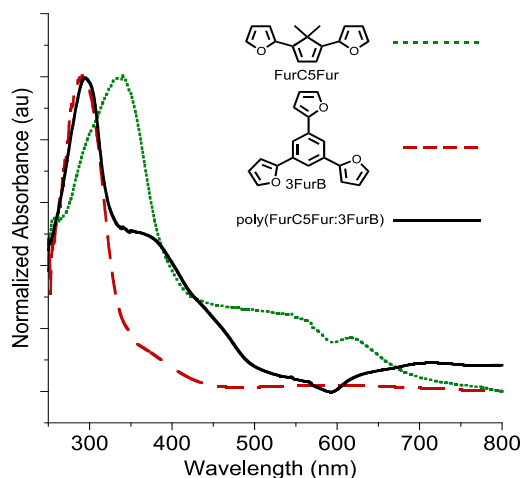


Figure 2-9: UV/vis absorbance spectra of FurC5Fur (drop casted film on ITO), 3FurB (drop casted film on ITO), and poly(FurC5Fur:3FurB) (electrochemically generated film on ITO).

Poly(FurC5Fur:3FurB) possesses a π - π^* transition band with a λ_{max} of 294 nm (Figure 2-9) which is blue-shifted by *ca.* 46 nm and 22 nm from the λ_{max} of FurC5Fur and 3FurB, respectively. The UV/vis of poly(FurC5Fur:3FurB) shows a low energy shoulder in line with the λ_{max} observed for FurC5Fur. The λ_{max} of poly(FurC5Fur:3FurB) is very close to the λ_{max} of the cross-linker, 3FurB. These features in the UV/vis spectrum support that both FurC5Fur and 3FurB are incorporated into the film. The absorption spectrum of the furan-containing system differs from the thiophene- and pyrrole-containing systems. In the thiophene and pyrrole systems the high energy shoulder in the UV/vis spectra is attributed to their respective 3XB cross-linking unit while the λ_{max} is in line with their XC5X repeat unit. However, for the furan system, the λ_{max} is attributed to 3FurB while the shoulder which is low energy is in line with FurC5Fur. Poly(FurC5Fur:3FurB) has a λ_{max} that is blue-shifted by *ca.* 12 nm compared to the homopolymer, poly(FurC5Fur), which is attributed to the use of a meta-substituted cross-linker that is expected to decrease the conjugation length.

2.4: Spectroelectrochemistry of poly(XC5X:3XB)

Spectroelectrochemical analyses on poly(XC5X:3XB) films grown on ITO were performed and are shown in Figures 2-6e-g with the results compared against poly(XC5X) where applicable. Poly(ThC5Th:3ThB) exhibits formation of two charge-carrier bands at *ca.* 786 and 884 nm upon the onset of oxidation that coalesce into a single band at higher potentials with a λ_{max} at *ca.* 866 nm. Poly(ThC5Th) has a broader transition than that observed in poly(ThC5Th:3ThB) which suggests that there is a smaller contribution from the superposition of the low energy absorption bands in poly(ThC5Th:3ThB). The oxidized films of poly(FurC5Fur:3FurB) have an even smaller contribution from the superposition of the low energy absorption bands with a series of well-defined charge-carrier transitions observed (Figure 2-6g) compared to the broad low energy absorption band present in doped films of the homopolymer, poly(FurC5Fur). The oxidation of poly(FurC5Fur:3FurB) films resulted in minimal bleaching of the π - π^* transition band due to the low conductivity of the film which is consistent with what has been observed. The data suggest that the poly(XC5X) homopolymers^{14f} possess a larger number of absorbing species with varying conjugation length compared to the doped copolymers which possess a limited number of absorbing species. This result is attributed to the presence of cross-linking 3XB junctions that would limit the number of charge-carrier types generated upon oxidation due to its meta-substituted arrangement. The neutral films of the thiophene and furan-containing polymers undergo complete reduction, while films of poly(PyrC5Pyr:3PyrB) possess a broad absorption band at *ca.* 694 nm (Figure 2-6f) that is indicative of incomplete reduction upon polymer film formation. As the film undergoes progressively higher potentials, the intensity of this

band increases and shifts to *ca.* 760 nm, a value that is red-shifted from its thiophene-containing congener.

2.5: Compositional Variation of Copolymers

Insoluble copolymer films were achieved using the molar ratio of 60:40 XC5X:3XB. By varying the comonomer feed ratio we can determine how the amount of 3XB affects the growth characteristics and optical properties of electrochemically-generated poly(XC5X:3XB) films. Comonomer molar ratios of 60:40, 75:25 and 90:10 (in the feed) for ThC5Th:3ThB were surveyed with subsequent copolymer films compared to the homopolymer poly(ThC5Th). In addition to ThC5Th being examined, its aromatic congener terthiophene (Th₃) was used for a compositional variation study.

The cyclic voltammograms of ThC5Th:3ThB copolymerizations (Figure 2-10) are similar to one another with the exception that anodic peak currents assigned to ThC5Th oxidation (*ca.* 0.5V, first scan) increase more rapidly (upon successive sweeps) with increasing ThC5Th:3ThB molar ratios.

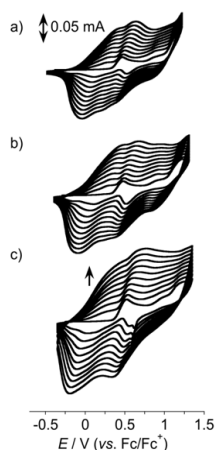


Figure 2-10: CV scans (10 cycles) of ThC5Th:3ThB at molar ratios: a) 60:40, b) 75:25, and c) 90:10. Conditions: concentration of electropolymerizable species, 4.2 mM in 0.1 M [n-Bu₄N]PF₆ in DCM; scan rate, 100 mV/s, Pt disc working electrode, *E* vs. Fc/Fc⁺.

Interestingly, the onset potential, E_{on} ca. -0.10 V, was the same for all the compositions of poly(ThC5Th:3ThB) in this study. These onset potentials were 100 mV lower than the homopolymer. In the same order, an increase in both $E_{\text{p,a}}$ (Table A-1) and degree of hysteresis in CV traces obtained from copolymer films deposited on Pt-disc electrodes (in monomer-free electrolyte solution) was also observed (Figure 2-11). This behavior could be attributed to requiring greater overpotentials to accommodate penetration of electrolyte and film reorganization during charge cycling,^{41b} due to more densely packed copolymer chains on the surface of the working electrode. These features have also been observed in other electrochemically-generated systems such as methano[10]annulene-thiophene random copolymers,^{14e} and oligothiophenes.⁴⁹

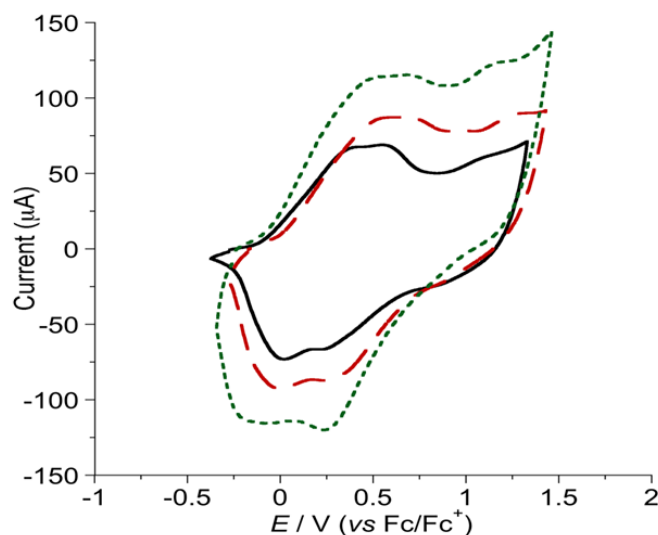


Figure 2-11: CV scans (in monomer-free electrolyte) of poly(ThC5Th:3ThB) films (deposited onto platinum disc electrodes) grown from comonomer solution with molar ratios: a) 60:40 (black line), b) 75:25 (red, long dash line), and c) 90:10 (green, short dash line).

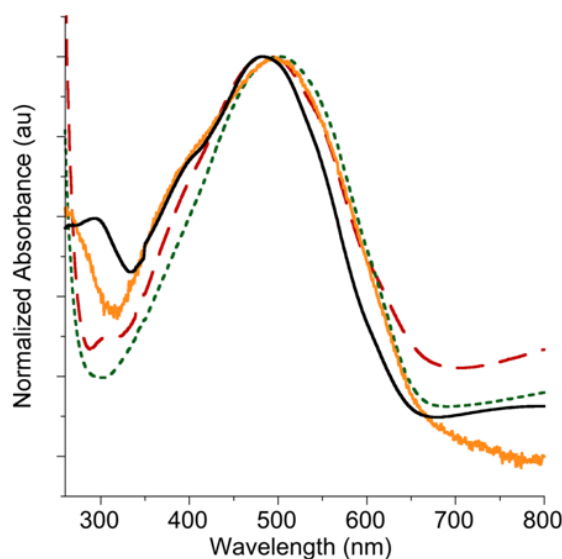


Figure 2-12: UV/vis absorbance spectra of poly(ThC5Th:3ThB) films (grown on ITO) prepared from comonomer solutions at molar ratios of 60:40 (black solid line), 75:25 (red long dash line), and 90:10 (green, short dash line). For comparison, the UV/vis absorbance spectrum of poly(ThC5Th) is shown as well (orange solid line).

As the ThC5Th:3ThB molar ratio of the comonomer solution increases in ThC5Th character, the λ_{max} of copolymer films deposited on ITO becomes more red-shifted (60:40, $\lambda_{\text{max}} = 482$ nm; 75:25, $\lambda_{\text{max}} = 487$ nm; and 90:10, $\lambda_{\text{max}} = 502$ nm, Figure 2-12).

This trend is to be expected when less meta-substituted cross-linker is available in the bulk solution since having meta-linkages in the polymer decreases the effective conjugation length. The λ_{max} of the 90:10 poly(ThC5Th:3ThB) was very close to the λ_{max} of the homopolymer poly(ThC5Th). (90:10, $\lambda_{\text{max}} = 502$ nm vs. poly(ThC5Th), $\lambda_{\text{max}} = 500$ nm) Moreover, the spectroelectrochemical profiles of these films (Figure 2-13) exhibit features in both the reduced and oxidized state that are more akin to poly(ThC5Th) when less 3ThB is employed in the comonomer feed.

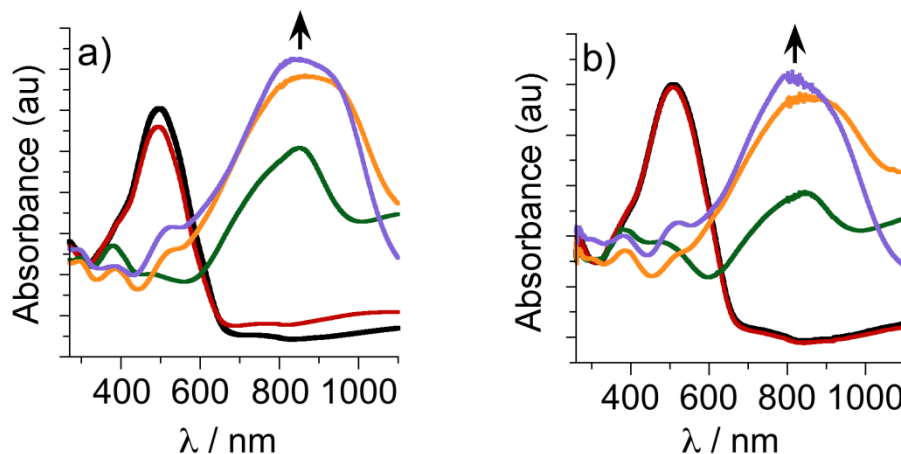


Figure 2-13: Spectroelectrochemical profiles of poly(ThC5Th:3ThB) prepared from comonomer solutions at molar ratios of (a) 75:25, and (b) 90:10. All black UV/Vis/NIR spectra were taken from films in their neutral state. All subsequent spectra (*i.e.* red, green, orange, violet, black dashed, and red dashed lines) were taken at progressively higher potentials at 200 mV intervals over the range of *ca.* -0.1 V and 1.1 V (E vs. Fc/Fc^+).

The spectroelectrochemical profiles of all the poly(ThC5Th:3ThB) films show bleaching of the π - π^* transition band and the progressive growth of a charge-carrier band *ca.* 800 nm as higher potentials are applied to the film. From the electrochemical data, these results indicate that copolymers possess a more extended chain structure between cross-linked junctions when less 3ThB is available in the comonomer solution during copolymerization. Therefore, only a limited amount of cross-linking agent is required to enhance film formation without compromising the properties exhibited by the homopolymer.

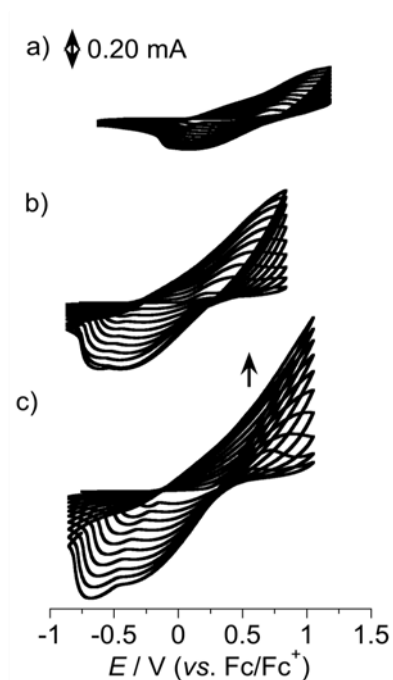


Figure 2-14: CV scans (10 cycles) of Th₃:3ThB at molar ratios: a) 60:40, b) 75:25, and c) 90:10. Conditions: concentration of electropolymerizable species, 4.2 mM in 0.1 M [*n*-Bu₄N]PF₆ in DCM; scan rate, 100 mV/s, Pt disc working electrode, *E* vs. Fc/Fc⁺.

Comparatively, the aromatic Th₃:3ThB sample set exhibits the same copolymer growth trend (Figure 2-14) observed in the ThC5Th:3ThB systems, however, the currents generated during copolymerization of Th₃:3ThB are much larger. This larger current ultimately leads to thicker films (60:40, 230 ± 40 nm, 75:25, 268 ± 135 nm, and 90:10, 366 ± 115 nm) when compared to their cyclopentadiene-containing analogues. The poly(Th₃:3ThB) films also possess a near identical UV/vis absorption spectra (Figure 2-15) with a λ_{max} of 368 nm for all compositions, followed by a succession of low-energy shoulders that are also present in spectra of electrochemically-generated poly(terthiophene).¹⁹ The charged oligothiophene species are not as soluble as those found in the diene-containing congeners because the bulk solutions of the terthiophene

system did not become darker during copolymerization. This resulted in more effective polymer deposition at the surface of the working electrode and is consistent with the electrochemical data obtained from ThC5Th and terthiophene.³³ The onset potential, E_{on} , of poly(Th₃:3ThB) films deposited on Pt disc electrodes are *ca.* 200 mV larger than the onset potential of the poly(ThC5Th:3ThB) systems. These results suggest that supplanting thiophene repeat units with cyclopentadiene alternatives can reduce the HOMO energy level and optical band gap in electrochemically-generated π -conjugated systems.

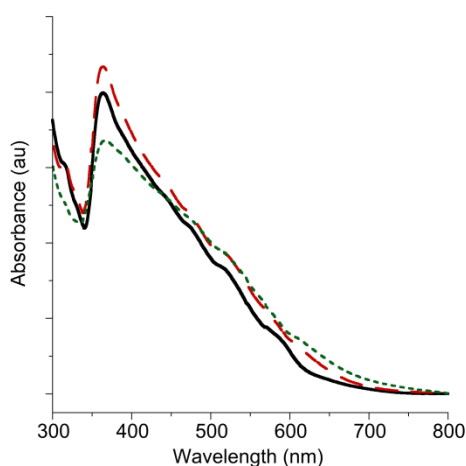


Figure 2-15: UV/vis absorbance spectra of poly(Th₃:3ThB) films (grown on ITO) prepared from comonomer solutions at molar ratios of 60:40 (black solid line), 75:25 (red long dash line), and 90:10 (green, short dash line).

Spectroelectrochemical analysis of the poly(Th₃:3ThB) copolymer films was performed and the results illustrated in Figure 2-16. At moderate doping levels, all films show a low energy band upon oxidation that is similar to the equivalent charge-carrier bands observed in the poly(ThC5Th:3ThB) systems, albeit blue-shifted by *ca.* 150 to 200 nm. After extensive doping, these bands begin to adopt a more broad and featureless shape when compared to poly(ThC5Th:3ThB). This shape is consistent with

homopolymers prepared from (oligo)thiophenes which indicates that poly(Th₃:3ThB) films are more likely to be rich in Th₃ than poly(ThC5Th:3ThB) films are in ThC5Th. The terthiophene system exhibits more efficient polymer deposition which gives rise to polymer segments that possess conjugation lengths that are comparable to those seen in poly(terthiophene) between cross-linking junctions.

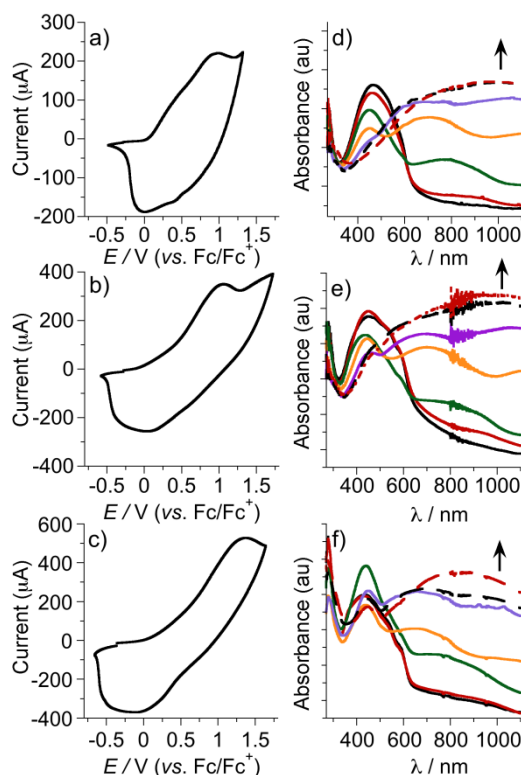


Figure 2-16: CV scans (in monomer-free electrolyte) of poly(Th₃:3ThB) prepared from comonomer solutions at molar ratios of (a) 60:40, (b) 75:25, and (c) 90:10. Spectroelectrochemical profiles of poly(Th₃:3ThB) prepared from comonomer solutions at molar ratios of (d) 60:40, (e) 75:25, and (f) 90:10. All black UV/Vis/NIR spectra were taken from films in their neutral state. All subsequent spectra (*i.e.* red, green, orange, violet, black dashed, and red dashed lines) were taken at progressively higher potentials at 200 mV intervals over the range of *ca.* 0.3 V and 1.3 V (*E* vs. Fc/Fc⁺).

2.6: Polymer Films and Morphology

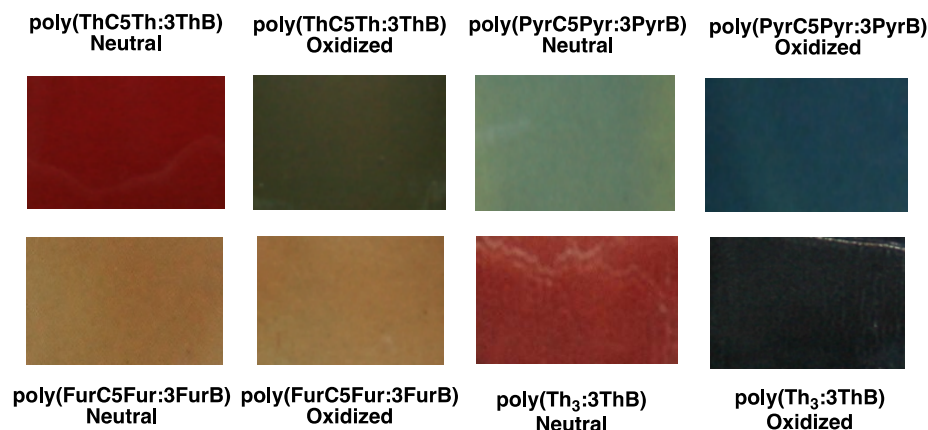


Figure 2-17: Thin-films of poly(XC5X:3XB) in the oxidized and reduced state deposited on ITO grown from 60:40 XC5X:3XB comonomer solutions.

Photos of the (XC5X:3XB) films in their neutral and oxidized state prepared from 60:40 comonomer solutions are shown in Figure 2-17. The color of the undoped copolymers is dependent on the aryl group employed in the comonomer system and spans from red to a green/blue. Poly(Th₃:3ThB) films are black in their oxidized state which is consistent with the spectroscopic data above due to the charge-carrier absorption band covering the entire visible spectrum. The oxidized films of poly(ThC5Th:3ThB) and poly(PyrC5Pyr:3PyrB) become darker but still have a distinctive color associated with them due to more narrow charge-carrier bands that are less absorbing in the blue region of the optical spectrum. The color of oxidized and neutral films of poly(FurC5Fur:3FurB) are nearly identical due to the poor formation of charge-carriers during oxidation as illustrated in Figure 2-6g. To investigate the morphology of the copolymer films a scanning electron microscopy was used with the micrographs illustrated in Figures 2-18.

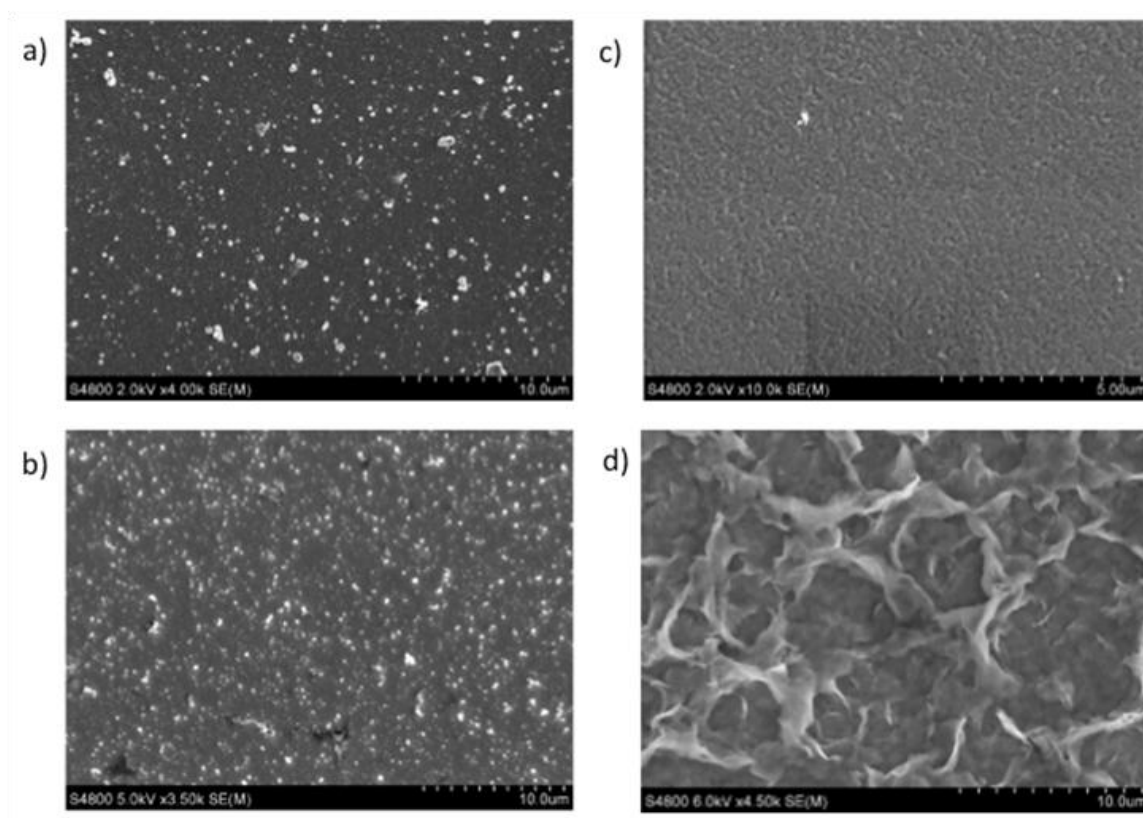


Figure 2-18: SEM micrographs of a) poly(ThC5Th:3ThB), b) poly(PyrC5Pyr:3PyrB), c) poly(FurC5Fur:3FurB), and d) poly(Th₃:3ThB) films deposited on ITO electrodes.

Poly(XC5X:3XB) films possess a homogenous surface covering the entire ITO surface and a dense and roughly packed assembly of polymer microstructures with a mound-like morphology. Poly(ThC5Th:3ThB) and poly(PyrC5Pyr:3PyrB) films possess larger microstructures compared to the furan congener due to more facile polymer growth observed in those systems. The films of poly(FurC5Fur:3FurB) have virtually no features except for a few mounds scattered throughout the film. Poly(Th₃:3ThB) films possess a laminar porous-like morphology that is typically seen in electrochemically-generated poly(thiophene)⁵⁰ films. This indicates that the cyclopentadiene moiety also influences the morphology of the films deposited on ITO electrodes due to the laminar morphology

seen in the aromatic congener versus the homogenous/mound-like morphology seen in the cyclopentadiene systems.

2.7: Conclusions

The electrochemical polymerization of 1,4-di(aryl)-5,5-dimethylcyclopentadienes bearing different aryl groups (*i.e.* thienyl, furyl, and *N*-methylpyrrolyl) was presented. The monomer-electrolyte solutions turned a dark color during polymerization for all the homopolymer systems, indicating that the oxidatively-coupled oligomers are too soluble for efficient polymer deposition at the surface of the working electrode. In order to improve film growth, XC5X monomers needed to be copolymerized with the cross-linking agent, 1,3,5-tris(2-aryl)benzenes. The addition of this cross-linker into the comonomer solution improved the film growth for all the monomers especially for the PyrC5Pyr:3PyrB system where no film was deposited onto the working electrode for the homopolymer. The optical, electronic, and spectroelectrochemical properties of the copolymer films were found to be aryl group-dependent. The ThC5Th:3ThB copolymers showed the lowest energy transitions in the neutral and doped states among the series. A compositional variation study of the comonomer molar ratio for the diene-containing system, ThC5Th, and the fully aromatic system, Th₃, was performed. This study revealed that as the molar ratio of the ThC5Th:3ThB comonomer solution increases in ThC5Th character, the properties of the thin film approach those observed for the homopolymer poly(ThC5Th) while utilizing 3ThB to improve film growth. The ThC5Th-containing polymer films possess absorption maxima and E_{on} values that are shifted to lower energies when compared to its all-aromatic congeners. This confirms that cyclopentadiene-containing polymers can reduce the optical band gap and HOMO energy

levels in electrochemically-generated polymer films when supplanting an aromatic repeat unit. This work offers insight into experimental design criteria that will enable the electrochemical synthesis of new π -conjugated organic polymers that are otherwise inaccessible due to the solubility issues that prevent polymer film formation without affecting the properties seen in the homopolymer.

2.8: Experimental and Methods

2.8.1: Materials and Equipment

All reactions were conducted under a dinitrogen atmosphere. All reagents were purchased from either Sigma Aldrich or VWR and used as received unless otherwise noted. Indium Tin Oxide (ITO) deposited on glass (Resistivity, 4-10 Ω) was purchased from Delta Technologies Ltd. Tetrabutylammonium hexafluorophosphate ($[n\text{-Bu}_4\text{N}]\text{PF}_6$) was recrystallized from absolute ethanol (2X) and dried *in vacuo* prior to use. Tetrahydrofuran (THF) and dichloromethane (DCM) were dried and collected from a PureSolv MD solvent purification system (Innovative Technology, Inc.) equipped with two activated alumina columns. Compounds XC5X (X = Th, Fur, Pyr)¹⁴ were prepared according to literature procedures. The synthesis of 3XB (X = Pyr, Fur)⁵¹ was prepared based on a procedure found in the literature for 3ThB. UV-Vis-NIR absorption spectra were recorded on a Cary-5000 spectrophotometer. ^1H and ^{13}C NMR spectra were recorded on a Varian INOVA spectrometer and calibrated to the residual protonated solvent at $\delta = 5.32$ and 54.00 respectively for deuterated methylene chloride (CD_2Cl_2). GC-MS experiments were conducted on an Agilent Technologies HP6890 GC system and 5973A MSD. Thin-film thickness was determined by atomic force microscopy using a Nanoscope IIIa Multimode scanning probe microscope. Measurements were taken on three different areas of the film. As such, thin-film thickness is expressed as a mean with standard deviation ($n = 3$). Scanning electron micrographs were taken by a Hitachi S-4800 field emission scanning electron microscope.

2.8.2: Electrochemistry

Cyclic voltammetry experiments were conducted with the use of a Metrohm AUTOLAB PGSTAT302N potentiostat/galvanostat. All experiments were performed in a single compartment cell using a platinum disk (*ca.* 3 mm²) working electrode, platinum mesh counter electrode, and silver wire reference electrode at a scan rate of 100 mV/s. Anhydrous [*n*-Bu₄N]PF₆ (0.1 M in DCM) was used as the supporting electrolyte. Comonomer solutions were prepared such that the concentration of electropolymerizable species was *ca.* 4.2 mM. Decamethylferrocene was used as an internal standard (half wave potential, $E_{1/2} = -0.59$ V) to adjust measured potentials relative to Fc/Fc⁺.⁵² Thin films for spectroelectrochemical analysis were grown by sweeping the working electrode (ITO deposited on glass) between appropriate potentials for a total of 5 cycles.

2.8.3: Spectroelectrochemistry

A polymer modified ITO working electrode, platinum mesh counter electrode, and silver foil reference electrode were placed in a quartz cuvette charged with electrolyte solution ([*n*-Bu₄N]PF₆ (0.1 M in DCM)) and loaded into a UV-Vis-NIR spectrophotometer. The working electrode was oxidized at a fixed potential for 180 s during which time an optical absorption spectrum was taken. The film was then reduced back to its neutral state and a second absorption spectrum taken to ensure that no damage to the film had occurred prior to subsequent experiments. The process was repeated at progressively higher positive potentials.

2.8.4: Synthesis of 1,3,5-Tris(2'-*N*-methylpyrrolyl)benzene (3PyrB)

A 2 M K₂CO₃ aq. solution (*ca.* 40mL) containing Pd(PPh₃)₂Cl₂ (26 mg, 0.036 mmol) was added via syringe to a Schlenk flask charged with 1,3,5-tribromobenzene

(0.25 g, 0.79mmol), 1-methyl-2-pyrroleboronic acid pinacol ester (0.82 g, 3.97 mmol) and anhydrous THF (*ca.* 55 mL). After 40 hours of refluxing, the solution was cooled to room temperature and quenched with a saturated solution of ammonium chloride. The organic contents of the flask were then extracted (3X) with CH₂Cl₂. The organic phase was collected, washed with brine, and dried over anhydrous Na₂SO₄. After filtration, the solvent was removed in vacuo and purified via a column chromatography (silica, hexanes) to afford a light brown solid (0.171g, yield, 69%). ¹H-NMR (CD₂Cl₂, 500 MHz): δ 3.75 (9H, s), 6.19 (3H, m), 6.28 (3H, m), 6.76 (3H, m), 7.39 (3H, s). ¹³C-NMR (CD₂Cl₂, 100 MHz): δ 35.95, 108.22, 109.75, 124.39, 127.01, 134.13, 134.45. GC/MS: m/z(%): 315 (100%) [M⁺]. Anal. Calcd. for C₂₁H₂₁N₃: C, 79.97; H, 6.71; N, 13.32. Found: C, 79.61; H, 6.71; N, 13.02.

Appendix

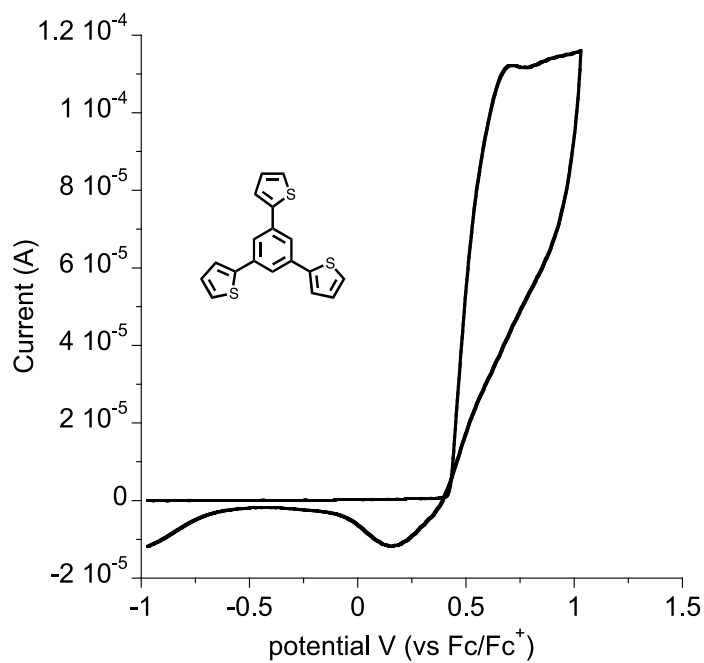


Figure A-1: Cyclic voltammogram of 3ThB [4.2 mM]. Conditions: 0.1 M [*n*-Bu₄N]PF₆ in DCM; scan rate, 100 mV/s, Pt disc working electrode, *E* vs. Fc/Fc⁺.

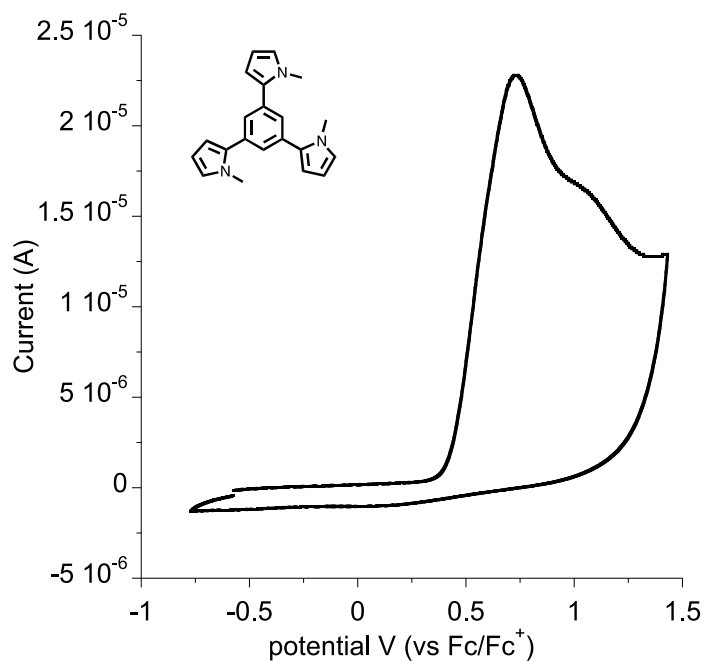


Figure A-2: Cyclic voltammogram of 3PyrB [4.2 mM]. Conditions: 0.1 M [*n*-Bu₄N]PF₆ in DCM; scan rate, 100 mV/s, Pt disc working electrode, *E* vs. Fc/Fc⁺.

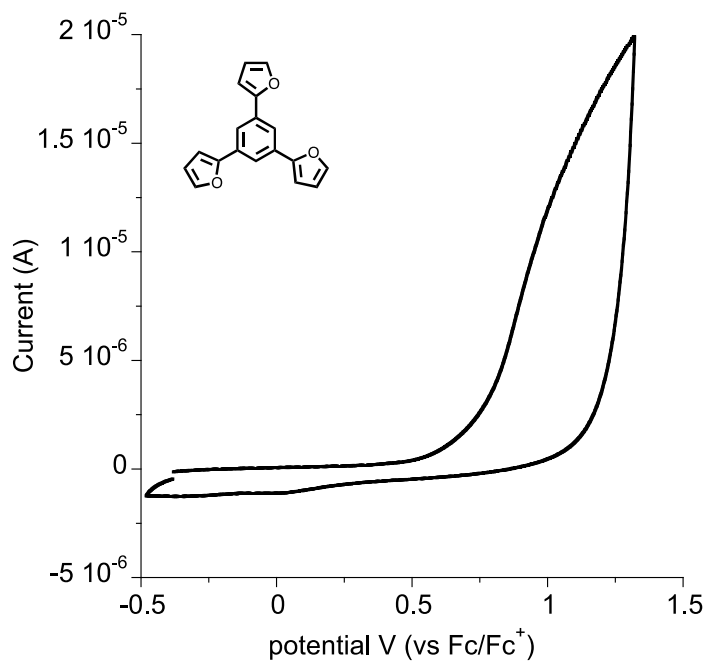


Figure A-3: Cyclic voltammogram of 3FurB [4.2 mM]. Conditions: 0.1 M [*n*-Bu₄N]PF₆ in DCM; scan rate, 100 mV/s, Pt disc working electrode, *E* vs. Fc/Fc⁺.

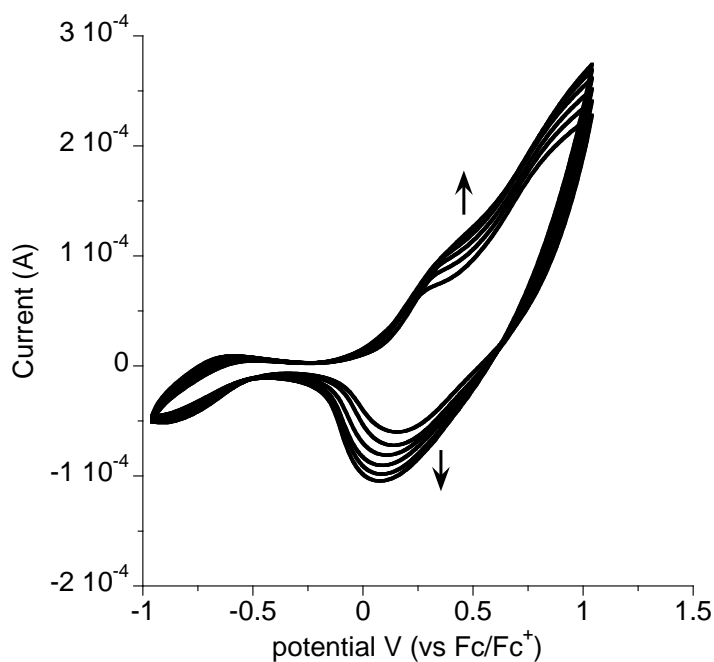


Figure A-4: Cyclic voltammogram of 3ThB [4.2 mM] (10 sweeps). Conditions: 0.1 M [*n*-Bu₄N]PF₆ in DCM; scan rate, 100 mV/s, Pt disc working electrode, *E* vs. Fc/Fc⁺.

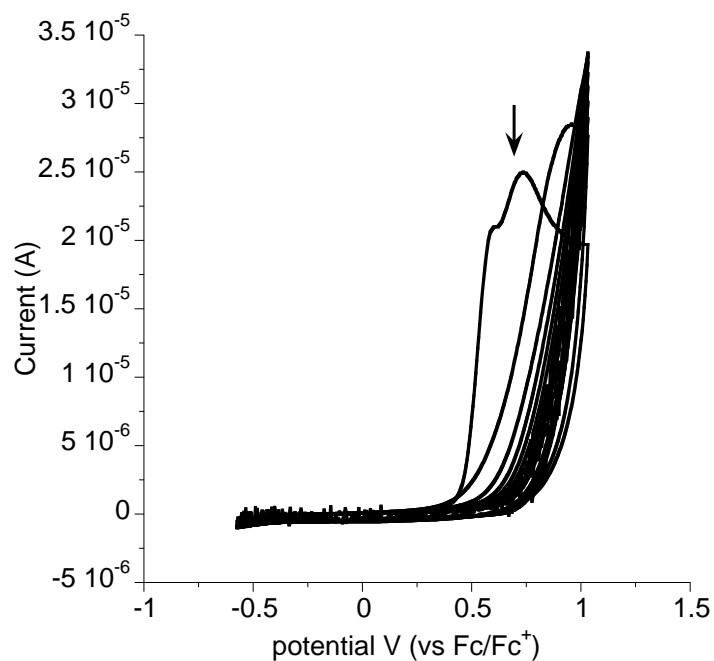


Figure A-5: Cyclic voltammogram of 3PyrB [4.2 mM] (10 sweeps). Conditions: 0.1 M $[n\text{-Bu}_4\text{N}]\text{PF}_6$ in DCM; scan rate, 100 mV/s, Pt disc working electrode, E vs. Fc/Fc^+ .

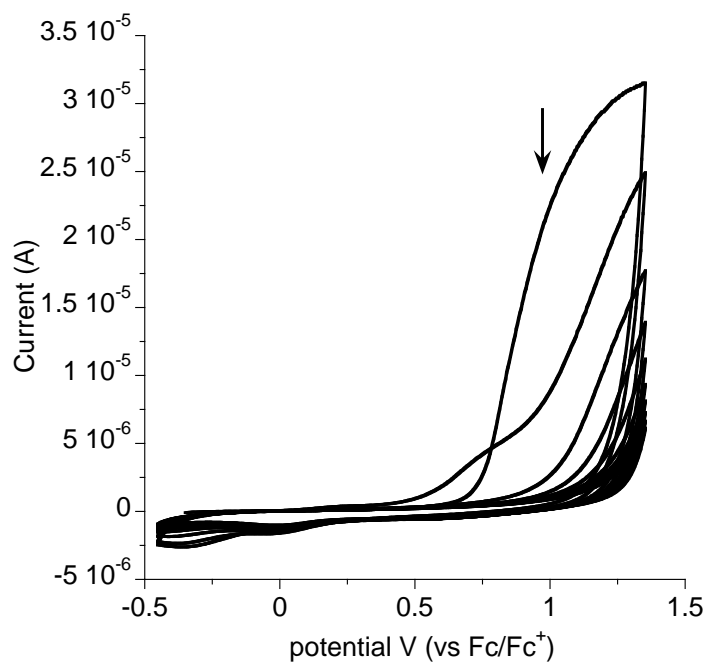


Figure A-6: Cyclic voltammogram of 3FurB [4.2 mM] (10 sweeps). Conditions: 0.1 M $[n\text{-Bu}_4\text{N}]\text{PF}_6$ in DCM; scan rate, 100 mV/s, Pt disc working electrode, E vs. Fc/Fc^+ .

Table A-1: (Co)polymer and monomer E_{on} and $E_{\text{p,a}}$ values.^a

Compound	E_{on} (V)	$E_{\text{p,a}}$ (V)
ThC5Th	0.32	1.27
3ThB	0.42	0.70
PyrC5Pyr	-0.09	0.35
3PyrB	0.40	0.72
FurC5Fur	0.19	1.55
3FurB	0.72	-
poly(ThC5Th:3ThB) 60:40	-0.10	0.54
poly(PyrC5Pyr:3PyrB) 60:40	-0.18	0.20
poly(FurC5Fur:3FurB) 60:40	0.00	0.30
poly(ThC5Th:3ThB) 75:25	-0.10	0.63
poly(ThC5Th:3ThB) 90:10	-0.10	0.70
poly(Th ₃ :3ThB) 60:40	0.24	0.63
poly(Th ₃ :3ThB) 75:25	0.24	1.05
poly(Th ₃ :3ThB) 90:10	0.24	1.43

^a 0.1 M [*n*-Bu₄N]PF₆ in DCM; scan rate, 100 mV/s, Pt disc working electrode, E vs. Fc/Fc⁺.

Chapter 2.9: References

- ¹ Menard, E.; Meitl, M. A.; Sun, Y.; Park, J.-U.; Shir, D. J.-L.; Nam, Y.-S.; Jeon, S.; Rogers, J. A. *Chem. Rev.* **2007**, *107*, 1117-1160.
- ² (a) Veinot, J. G. C.; Marks, T. J. *Acc. Chem. Res.* **2005**, *38*, 632-643. (b) Karl, N. In *Organic Electronic Materials: Conjugated Polymers and Low Molecular weight Organic Solids*; Farchioni, R., Grosso, G., Eds.; Springer-Verlag: Berlin, 2001; Pp 215-240.
- ³ Beaujuge, P. M.; Reynolds, J.R. *Chem. Rev.* **2010**, *110*, 268-320.
- ⁴ Thomas, S. W., III; Joly, G. D.; Swager, T. M. *Chem. Rev.* **2007**, *107*, 1339-1386. (b) McQuade, D. T.; Pullen, A. E.; Swager, T. M. *Chem. Rev.* **2000**, *100*, 2537-2574.
- ⁵ Cheng, Y.-J.; Yang, S.-H.; Hsu, C.-S. *Chem. Rev.* **2009**, *109*, 5868-5923.
- ⁶ Zhang, Q.; Sun, Y.; Xu, W.; Zhu, D. *Adv. Mater.* **2014**, *26*, 6829-6851.
- ⁷ Shirakawa, H.; Louis, E. J.; MacDiarmid, A.G.; Chiang, C.K.; Heeger, A.J. *J Chem Soc Chem Comm.* **1977**, 578-580.
- ⁸ "The Nobel Prize in Chemistry 2000". *Nobelprize.org*. Nobel Media AB 2014. Web. 26 Jan 2015. <http://www.nobelprize.org/nobel_prizes/chemistry/laureates/2000/>
- ⁹ Chiang, C. K.; Fincher, Jr., C. R.; Park, Y. W.; Heeger, A. J.; Shirakawa, H.; Louis, E. J. *Phys. Rev. Lett.* **1977**, *39*, 1098.
- ¹⁰ Jones, L. C., Jr.; Taylor, L. W. *Anal. Chem.* **1955**, *27*, 228.
- ¹¹ (a) Roncali, J. *Macromol. Rapid Commun.* **2007**, *28*, 1761-1775. (b) Arias, A. C.; MacKenzie, J. D.; McColloch, I.; Rivnay, J.; Salleo, A. *Chem. Rev.* **2010**, *110*, 3-24. (c) Krebs, F. C.; *Sol. Energy Mater. Sol. Cells* **2009**, *93*, 394-412.
- ¹² (a) Brédas, J. -L.; Thémans, B.; Fripiat, J. G.; André, J. M.; Chance, R. R. *Phys. Rev. B.* **1984**, *29*, 6761-6773. (b) Lee, Y. -S.; Kertesz, M. *J. Chem. Phys.* **1988**, *88*, 2609-2617.
- ¹³ Wong, B.M.; Cordaro, J.G. *J. Phys. Chem.* **2011**, *115*, 18333-18341.
- ¹⁴ (a) Azoulay, J. D.; Koretz, Z. A.; Wong, B. M.; Bazan, G. C. *Macromolecules* **2013**, *46*, 1337-1342. (b) Coppo, P.; Cupertino, D. C.; Yeates, S. G.; Turner, M. L. *Macromolecules* **2003**, *36*, 2705-2711. (c) Lambert, T. L.; Ferraris, J. P. *J. Chem. Soc., Chem. Commun.* **1991**, 752-754. (d) Ferraris, J. P.; Lambert, T. L. *J. Chem. Soc., Chem. Commun.* **1991**, 1268-1270. (e) Elbaz, G. A.; Repka, L. M.; Tovar, J. D. *ACS Appl. Mater. Interfaces*, **2011**, *3*, 2551-2556. (f) Peart, P. A.; Tovar, J. D. *Org. Lett.*, **2007**, *9*, 3041-3044.
- ¹⁵ Roncali, J. *Chem. Rev.* **1992**, *92*, 711-738.
- ¹⁶ González-Tejera, M.J.; Sánchez de la Blanca, E.; Carrillo, I. *Synth. Met.* **2008**, *158*, 165-189.
- ¹⁷ Miller, J. S. In "Extended Linear Chain Compounds," Vol. 3, Diaz, A. F.; Kanazawa, K. K. J., Ed., Plenum Press: New York, 1983; pp 417-440.
- ¹⁸ Visy, C.; Lukkari, J.; Kankare, J. *Macromolecules* **1994**, *27*, 3322-3329.
- ¹⁹ Roncali, J.; Garnier, F.; Lemaire, M. Garreau, R. *Synth. Met.* **1986**, *15*, 323-331.
- ²⁰ Tourillon, G.; Garnier, F. *J. Phys. Chem.* **1983**, *87*, 2289.
- ²¹ Waltman, R. J.; Bargon, J.; Diaz, A. F.; *J. Phys. Chem.* **1983**, *87*, 1459.
- ²² Roncali, J.; Garreau, R.; Yassar, A.; Marque, P.; Garnier, F.; Lemaire, M. *J. Phys. Chem.* **1987**, *31*, 127.

-
- ²³ Nessakh, B.; Kotkowska-Machnik, Z.; Tedjar, F. *J. Electroanal. Chem.* **1990**, 269, 263-268.
- ²⁴ Glenis, S.; Benz, M.; LeGoff, E.; Schindler, J. L.; Kannewurf, C. R.; Kanatzidis, M. *G. J. Am. Chem. Soc.* **1993**, 115, 12519-12525.
- ²⁵ Idzik, K. R.; Ledwon, P.; Beckert, R.; Golba, S.; Frydel, J.; Lapkowski, M.; *Electrochimica Acta*, **2010**, 55, 7419-7426.
- ²⁶ (a) Wudl, F.; Kobayashi, M.; Heeger, A. J. *J. Org. Chem.* **1984**, 49, 3382-3382, (b) Pomerantz, M.; Chaloner-Gill, B.; Harding, L. O.; Tseng, J. J.; Pomerantz, W. J. *J. Chem. Soc., Chem. Commun.* **1992**, 1672-1673. (c) Hong, S. Y.; Marynick, D. S. *Macromolecules* **1992**, 25, 4652-4657. (d) Sotzing, G. A.; Lee, K. *Macromolecules* **2002**, 35, 7281-7286.
- ²⁷ (a) Speros, J. C.; Martinez, H.; Paulsen, B. D.; White, S. P.; Bonifas, A. D.; Goff, P. C.; Frisbie, C. D.; Hillmyer, M. A. *Macromolecules* **2013**, 46, 5184-5194, (b) Frère, P.; Raimundo, J. -M.; Blanchard, P.; Delaunay, J.; Richomme, P.; Sauvajol, J. -L.; Orduna, J.; Roncali, J. *J. Org. Chem.* **2003**, 68, 7254-7265.
- ²⁸ Streifel, B. C.; Peart, P. A.; Hardigree Martínez, J. F.; Katz, H. E. Tovar, J. D. *Macromolecules* **2012**, 45, 7339-7349.
- ²⁹ Schleyer, P. v. R.; Manoharan, M.; Wang, Z.-X.; Kiran, B.; Jiao, H.; Puchta, R.; Hommes, N. J. R. v. E. *Org. Lett.* **2001**, 3, 2465-2468.
- ³⁰ (a) Günther, H. *NMR Spectroscopy: Basic Principles, Concepts, and Applications in Chemistry*, 2nd Ed.; Wiley: Chichester, 1995. (b) Martin, N. H.; Brown, D. *Int. J. Mol. Sci.* **2000**, 1, 84 and references cited.
- ³¹ Fleischer, U.; Kutzelnigg, W.; Lazzeretti, P.; Mühlenkamp, V. *J. Am. Chem. Soc.* **1994**, 116, 5298.
- ³² Schleyer, P. v. R.; Jiao, H.; Hommes, N. J. R. v. E.; Malkin, V. G.; Malkina, O. L. *J. Am. Chem. Soc.* **1997**, 119, 12669.
- ³³ Chen, L. Mahmoud, S. M.; Yin, X.; Lalancette, R. A.; Pietrangelo, A. *Org. Lett.* **2013**, 15, 5970-5973.
- ³⁴ (a) Seixas de Melo, J.; Elisei, F.; Gartner, C.; Aloise, G. G.; Becker, R. S.; *J. Phys. Chem. A* **2000**, 104, 6907-6911. (b) Kauffmann, T.; Lexy, H. *Chem. Ber.* **1981**, 114, 3667-3673.
- ³⁵ (a) Rohde, N.; Eh, M.; Geißler, U.; Hallensleben, M. L.; Voigt, B.; Voigt, M. *Adv. Mater.* **1995**, 7, 401-404. (b) Geißler, U.; Hallensleben, M. L.; Rohde, N. *Macromol. Chem. Phys.* **1996**, 197, 2565-2576. (c) Kauffmann, T.; Lexy, H. *Chem. Ber.* 1981, 114, 3674-3683.
- ³⁶ Chen, W.; Li, H.; Widawsky, J. R.; Appayee, C.; Venkataraman, L.; Breslow, R. *J. Am. Chem. Soc.* **2014**, 136, 918-920.
- ³⁷ For examples, see: (a) Poverenov, E.; Sheynin, Y.; Zamoshchik, N.; Patra, A.; Leitus, G.; Perepichka, I. F.; Bendikov, M. *J. Mater. Chem.*, **2012**, 22, 14645-14655. (b) Pietrangelo, A.; Sih, B. C.; Boden, B. N.; Wang, Z.; Li, Q.; Chou, K. C.; MacLachlan, M. J.; Wolf, M. O. *Adv. Mater.* **2008**, 20, 2280-2284. (c) Kawabata, K.; Takeguchi, M.; Goto, H. *Macromolecules* **2013**, 46, 2078-2091. (d) Kenning, D. D.; Rasmussen, S. C. *Macromolecules* **2003**, 36, 6298-6299.
- ³⁸ Abdou, M. S. A.; Lu, X.; Xie, Z. W.; Orfino, F.; Deen, M. J.; Holdcroft, S. *Chem. Mater.* **1995**, 7, 631-641.

-
- ³⁹ Berlin, A.; Zotti, G.; Zecchin, S.; Schiavon, G. *Macromol. Chem. Phys.* **2002**, *203*, 1228-1237.
- ⁴⁰ Zotti, G.; Schiavon, G. *Synth. Met.* **1990**, *39*, 183.
- ⁴¹ (a) Ferraris, J. P.; Hanlon, T. R. *Polymer* **1989**, *30*, 1319-1327. (b) Yassar, A.; Roncali, J.; Garnier, F. *Macromolecules* **1989**, *22*, 804-809.
- ⁴² Sharma, S.; Bendikov, M. *Chem. Eur. J.*, **2013**, *19*, 13127-13139.
- ⁴³ Politis, J. K.; Nemes, J. C.; Curtis, M. D. *J. Am. Chem. Soc.*, **2001**, *123*, 2537-2547.
- ⁴⁴ Patil, A. O.; Heeger, A. J.; Wudl, F.; *Chem. Rev.* **1988**, *88*, 183-200.
- ⁴⁵ Alkan, S.; Cutler, C. A.; Reynolds, J. R. *Adv. Funct. Mater.* **2003**, *13*, 331-336.
- ⁴⁶ Zhen, S.; Lu, B.; Xu, J.; Zhang, S.; Li, Y. *RSC Adv.* **2014**, *4*, 14001-14012.
- ⁴⁷ (a) Krische, B.; Zagorska, M. *Synth. Met.* **1989**, *28*, 263-268. (b) Marque, P.; Roncali, J.; Garnier, F. *J. Electroanal. Chem.* **1987**, *218*, 107-118.
- ⁴⁸ Wei, Y.; Chan, C. -C.; Tian, J.; Jang, G. -W.; Hsueh, K. F.; *Chem. Mater.*, **1991**, *3*, 888-897.
- ⁴⁹ Zotti, G.; Schiavon, G.; Berlin, A.; Pagani, G. *Chem. Mater.* **1993**, *5*, 620-624.
- ⁵⁰ Tourillon, G.; Garnier, F. *J. Polym. Sci., Polym. Phys. Ed.*, **1984**, *22*, 33-39.
- ⁵¹ Guan, L.; Zhao, X.-Q.; Zhong, Y.-P.; Liu, P.; Deng, W.-J. *Solid State Phenom.* **2012**, *181*, 237-240.
- ⁵² Connelly, N. G.; Geiger, W. E. *Chem. Rev.* **1996**, *96*, 877-910.

Curriculum Vitae

Michael E. Vega

Education

B.S., Chemistry University of Notre Dame
Minor, Chinese August 2008-May 2012

M.S., Chemistry Rutgers, The State University of New Jersey
Graduate School, Newark, NJ
September 2012- May 2015

Work Experience

GEA, Northvale, NJ December 2012 – March 2013
Warehouse Inventory
Shipping Department

Dawgpizza, Alumni Hall, University of Notre Dame, Notre Dame, IN, 2008-2012
Food preparation
Telephone orders
Cashier

Internship – Virology Laboratories, Hackensack University Medical Center,
Hackensack, NJ,
May 2011 – July 2011
Examined and reported Cytomegalovirus cultures
Updated laboratory procedure manuals

Men's & Women's Inter- Hall Lacrosse League, University of Notre Dame,
Notre Dame, IN, 2010 -2011
Game referee

Advanced Laparoscopic Associates, Hackensack, NJ, May 2008 - August 2008
Escorted patients to exam rooms, performed biometrics
Prepared and stocked exam rooms
Organized and filed medical records